Eur. Phys. J. C (2017) 77:338
DOI 10.1140/epjc/s10052-017-4893-7

THE EUROPEAN PHYSICAL JOURNAL C

Regular Article - Theoretical Physics

Improved predictions for intermediate and heavy supersymmetry in the MSSM and beyond

Florian Staub[1,2,a], **Werner Porod**[3]

[1] Institute for Theoretical Physics (ITP), Karlsruhe Institute of Technology, Engesserstraße 7, 76128 Karlsruhe, Germany
[2] Institute for Nuclear Physics (IKP), Karlsruhe Institute of Technology, Hermann-von-Helmholtz-Platz 1, 76344 Eggenstein-Leopoldshafen, Germany
[3] Institut für Theoretische Physik und Astronomie, Universität Würzburg, Am Hubland, 97074 Würzburg, Germany

Received: 23 March 2017 / Accepted: 5 May 2017 / Published online: 22 May 2017

Abstract For a long time, the minimal supersymmetric standard model (MSSM) with light masses for the supersymmetric states was considered as the most natural extension of the Standard Model of particle physics. Consequently, a valid approximation was to match the MSSM to the precision measurement directly at the electroweak scale. This approach was also utilized by all dedicated spectrum generators for the MSSM. However, the higher the supersymmetric (SUSY) scale is, the bigger the uncertainties which are introduced by this matching. We point out important consequences of a two-scale matching, where the running parameters within the SM are calculated at M_Z and evaluated up to the SUSY scale, where they are matched to the full model. We show the impact on gauge coupling unification as well as the SUSY mass spectrum. Also the Higgs mass prediction for large supersymmetric masses has been improved by performing the calculation within an effective SM. The approach presented here is now also available in the spectrum generator `SPheno`. Moreover, also `SARAH` was extended accordingly and gives the possibility to study these effects now in many different supersymmetric models.

1 Introduction

The discovery of the Higgs with a mass of about 125 GeV [1,2] is, to date, the biggest success of the large hadron collider (LHC). In contrast, there has not been any evidence for new physics. This puts very strong constraints on the masses of new coloured particles as predicted, for instance, by supersymmetry (SUSY); working with very simplified assumptions, it is possible to exclude gluinos and first/second generation squarks nearly up to 2 TeV [3–6]. These experimental results raise not only the question if minimal supersymmetry is still a good solution to the fine-tuning or hierarchy problem of the standard model of particle physics (SM), but also gives new challenges to study the MSSM precisely.

In the past many studies for the MSSM were done under the impression that the scale of supersymmetry, $M_{\rm SUSY}$, should be close to the electroweak scale M_Z. With this assumption it was possible to calculate the gauge couplings in the $\overline{\rm DR}$ scheme directly from m_Z, G_F and α_{em} as well as the $\overline{\rm DR}$ Yukawa couplings from the pole mass of the top quark and the running $\overline{\rm MS}$ lepton and light quark masses given at $Q = m_Z$. More importantly the Higgs masses have been calculated at fixed order in the full supersymmetric model. However, both calculations became less accurate the larger $M_{\rm SUSY}$ is because potentially large logarithms of form $\log \frac{M_{\rm SUSY}}{M_Z}$ and $\log \frac{M_{\rm SUSY}}{m_h}$, respectively, appear. Therefore, ongoing efforts are being made to improve the calculation in the presence of supersymmetric scales which are well above the electroweak one. The first road is to keep the current set-up in principle but improve it by higher order corrections: for instance, `SoftSUSY` provides the possibility to include higher order corrections to the threshold corrections at the weak scale and in the renormalisation group equation (RGE) running between the weak and SUSY scale, in order to get a better determination of the $\overline{\rm DR}$ parameters at the SUSY scale [7]. The first ansatz is to calculate the Higgs mass still in the full MSSM but extends the two-loop fixed order calculation by a resummation of potential large logarithm involving stops. That has been done for instance by `FeynHiggs` since a few years [8–10]. The second approach, which is becoming more and more popular, is to work in an effective theory below $M_{\rm SUSY}$: `SusyHD` [11] and recent versions of `FlexibleSUSY` [12] as well as `FeynHiggs` [13] can consider below $M_{\rm SUSY}$ only the degrees of freedom of the SM, and match the SM to the MSSM just at the SUSY scale. Also

[a] e-mail: florian.staub@kit.edu

the Higgs mass calculation is done in the effective SM by obtaining a value of the quartic Higgs coupling $\lambda_{\rm SM}$ from the matching between the MSSM and SM at $M_{\rm SUSY}$. The idea to work in an effective SM below $M_{\rm SUSY}$ was already well explored in literature before it became easily available via public tools; see e.g. Refs. [14–20]. Similarly, also a general Two-Higgs-Doublet-Model was already considered as low energy limit of the MSSM [21–23]. Finally, since several years Split-SUSY variants of the MSSM have become more and more popular in which the coloured SUSY particles are integrated out [15–17,24–26].

We have now also extended the stand-alone spectrum generator SPheno [27,28] as well as the Mathematica package SARAH [29–34], which gives the possibility to auto-generate a spectrum generator for a given model, to improve the predictions for moderate and heavy SUSY scales. Here, we made use of the second approach: the running $\overline{\rm DR}$ parameters at the SUSY scale are obtained via a two-scale matching procedure and the Higgs mass calculation can optionally be done within an effective SM. We give in the following not only details of our exact approach but discuss also phenomenological consequences of the improved calculations. We focus not only on the Higgs mass prediction, which has been already discussed to some extent in the recent year, but show also potential important effects on the SUSY mass spectrum. Beside the MSSM we consider also it is minimal extension, the NMSSM.

This paper is organised as follows: in Sect. 2 we summarize our approach to obtain the $\overline{\rm DR}$ parameters at the SUSY scale as well as to calculate the mass of the SM-like Higgs. Many details for the matching are given in Appendix Appendix A, where also the differences between stand-alone SPheno and the SARAH generated version are discussed. In Sect. 3 we discuss the numerical impact of the improved calculation on the running parameters, but also on the SUSY and Higgs masses in the MSSM and beyond. We conclude in Sect. 4.

2 Matching procedure and effective Higgs mass calculation

2.1 The two-scale matching in SARAH

So far, all dedicated MSSM spectrum generators such as SoftSUSY [7,35–37], Suspect [38] or SPheno were adapting the procedure of Ref. [39] to obtain the running gauge and Yukawa couplings at the SUSY scale. All details of the calculations are summarised in Appendix A.1. The principal idea is that all measured SM parameters are already translated at M_Z into $\overline{\rm DR}$ values taking into account the complete MSSM spectrum which are then evaluated to the SUSY scale by using the RGEs of the MSSM. This procedure suffers from increasing uncertainties when the separation of the electroweak and SUSY scale becomes large. In order to reduce the theoretical uncertainty for large SUSY scales, SoftSUSY is able since some time to include the two-loop SUSY thresholds in the calculation of the $\overline{\rm DR}$ parameters and to perform a three-loop RGE running between M_Z and $M_{\rm SUSY}$. With these additional corrections, potential large effects in the prediction of the higgsino mass parameter but also for the Higgs mass were found. The drawback of this ansatz is that it is computational very expensive and slows down the evaluation of a given parameter point significantly. Moreover, only the effects of a more precise determination of the top Yukawa coupling on the Higgs mass are caught in this approach up to some extent, while a still potential large logarithm in the fixed order Higgs mass calculation can be present.

Therefore, we shall use another ansatz in SPheno and SARAH[1] which is closer to the set-up of NMSSMCalc [40] or specific versions of FlexibleSUSY [12,41]: the matching at the electroweak scale includes only SM thresholds to obtain the $\overline{\rm MS}$ values of the gauge and Yukawa couplings and the electroweak vacuum expectation value (VEV). These parameters are then evolved up to the SUSY scale using SM RGEs, and the translation from $\overline{\rm MS}$ to $\overline{\rm DR}$ scheme and the inclusion of SUSY thresholds is done at the SUSY scale. All details of the calculation are given in Appendix A. The precision to obtain the $\overline{\rm DR}$ parameters at the SUSY scale via this two-scale matching (2SM) is as follows in SARAH/SPheno:

1. The $\overline{\rm MS}$ parameters at the weak scale are calculated using:
   - One-loop electroweak corrections to the fermion masses.
   - Two-loop QCD corrections to the top-quark mass.
   - One-loop corrections to δ_{VB} as well as one- and two-loop corrections to δ_ρ.
2. The SM RGEs are available up to three-loop order.
3. The $\overline{\rm MS}$–$\overline{\rm DR}$ conversion of the running fermion masses is done at two-loop α_s and at one-loop in the case of the electroweak gauge couplings.
4. The $\overline{\rm MS}$–$\overline{\rm DR}$ conversion of the gauge couplings is done at one-loop order.
5. The SUSY thresholds are included at full one-loop order.

The $\overline{\rm DR}$ parameters obtained in that way are then used to calculate the SUSY and Higgs masses at $M_{\rm SUSY}$. Since both, the matching at the M_Z and $M_{\rm SUSY}$ depends on these masses, one needs to iterate the matching procedure. For this reason it is necessary to calculate the quartic self-coupling

[1] We use in the following SARAH as synonym for 'a SARAH generated spectrum generator based on SPheno'.

$\lambda_{\rm SM}(M_{\rm SUSY})$ within the SM which is a function of the SUSY masses and parameters. A handy and very general ansatz to obtain $\lambda_{\rm SM}(M_{\rm SUSY})$ was presented in Ref. [12]: one can match the Higgs pole masses in the full MSSM and the SM at the SUSY scale

$$m_h^{\rm SM,pole}(M_{\rm SUSY}) \equiv m_h^{\rm MSSM,pole}(M_{\rm SUSY}), \tag{1}$$

from which one can derive $\lambda_{\rm SM}$:

$$\begin{aligned}(v^{\overline{\rm MS}}(M_{\rm SUSY}))^2\lambda_{\rm SM}(M_{\rm SUSY}) &= (m_h^{\rm SM,tree}(M_{\rm SUSY}))^2 \\ &= (m_h^{\rm MSSM,pole}(M_{\rm SUSY}))^2 - \Pi_h(M_{\rm SUSY}).\end{aligned} \tag{2}$$

Here, $\Pi_h(M_{\rm SUSY})$ are the radiative corrections to the Higgs mass within the SM which are calculated using $\overline{\rm MS}$ parameters at this scale, while the pole-mass calculation in the MSSM involves $\overline{\rm DR}$ parameters. The equivalence of this ansatz to the matching of four point function as for instance performed in Refs. [19,20] and used also by SUSYHD has been explicitly shown in Ref. [12]. SM RGEs are used afterwards to run $\lambda_{\rm SM}$ to M_Z, and the $\overline{\rm MS}$ parameters are recalculated at this scale. This procedure is iterated until the mass spectrum at the SUSY scale has converged.

2.2 Differences between SARAH and SPheno in the new matching routines

The above procedure corresponds to the details in SARAH whereas the procedure implemented in the stand-alone SPheno differs in the following details:

- at $Q = m_t$: the top Yukawa coupling is optionally replaced by the fit formula given by Eq. (57) of Ref. [42];
- at $Q = m_t$: the strong coupling g_3 is optionally replaced by the fit formula given by Eq. (60) of Ref. [42];
- at $Q = M_{\rm SUSY}$: the thresholds corrections to the gauge and Yukawa interactions are calculated in the electroweak basis assuming an unbroken $\mathrm{SU}(2)_L \times U(1)_Y$. The full formulae are given in Appendix A.

The flags to use/not to use with the fit formulae of Ref. [42] are given in Appendix A.2. If not indicated otherwise, these fit formulae are used in the following comparisons.

2.3 The effective Higgs mass calculation

So far, the mass calculation with SPheno/SARAH would have stopped after the conversion of the mass spectrum at $M_{\rm SUSY}$. However, this could lead to a large theoretical uncertainty in the Higgs mass prediction for large SUSY masses: the fixed order Higgs mass calculation as performed by SPheno/SARAH would become inaccurate because of the appearance of large logarithms $\sim \log(M_{\rm SUSY}/M_{ew})$. In order to cure this, one could do a resummation of these large logs. However, in our set-up it is much easier to use the value $\lambda_{\rm SM}(M_{\rm SUSY})$, which is already known, and run it to the top mass scale. By this running all large logarithms get re-summed and one can then calculate m_h at m_t within the SM including radiative corrections. In SARAH/SPheno we include the full SM one-loop corrections as well as the two-loop corrections $O(\alpha_t(\alpha_s\alpha_t))$ to m_h. The schematic procedure for the matching and Higgs mass calculation is summarized in Fig. 1.

3 Consequences of the two-scale matching & effective Higgs mass calculation

3.1 Running SM couplings

All the efforts to disentangle the weak and the SUSY scale in the matching are done to get more accurate values of the running $\overline{\rm DR}$ parameters at the SUSY scale. Therefore, we want to start the discussion of the impact of the new matching procedure with presenting the changes in the $\overline{\rm DR}$ parameters at the SUSY scale. The results for the top and bottom Yukawa couplings are shown in Fig. 2 and those for the three gauge couplings g_1, g_2 and g_3 are depicted in Fig. 3. Since the exact matching procedure using two scales is slightly different between SPheno and SARAH as explained in Sect. 2.2 we show the new results for both codes. Since we have turned off here the fit formula of Ref. [42] in the SPheno calculation, the remaining differences appearing here are due to the threshold corrections of the gauge and Yukawa couplings at $M_{\rm SUSY}$. One sees that in particular the top Yukawa coupling changes significantly compared to the older calculation with only one matching scale (1SM). For $M_{\rm SUSY} = 100$ TeV, the calculated $\overline{\rm DR}$ value with SARAH using the two-scale matching is nearly 10% below the one for the one-scale matching. These large changes are in agreement with the results of Ref. [12] where the impact of a 2SM on the top Yukawa coupling has also been addressed analytically. We show for comparison also the calculated couplings in SoftSUSY with and without two-loop SUSY thresholds and three-loop RGEs. It is obvious that there was a non-negligible difference between the old results and the one-loop results of SoftSUSY, although both calculations were of the same order in perturbation theory. The reason is the matching condition, which can schematically be written as

$$m_t^{\overline{\rm DR}} = m_t^{\rm pole} + \hat{m}_t\,\Sigma(\hat{m}_t^2), \tag{3}$$

where all loop corrections are summarised in Σ. SPheno uses $\hat{m}_t = m_t^{\overline{\rm DR}}$ while SoftSUSY and other codes set $\hat{m}_t = m_t^{\rm pole}$. The result obtained with the new two-scale

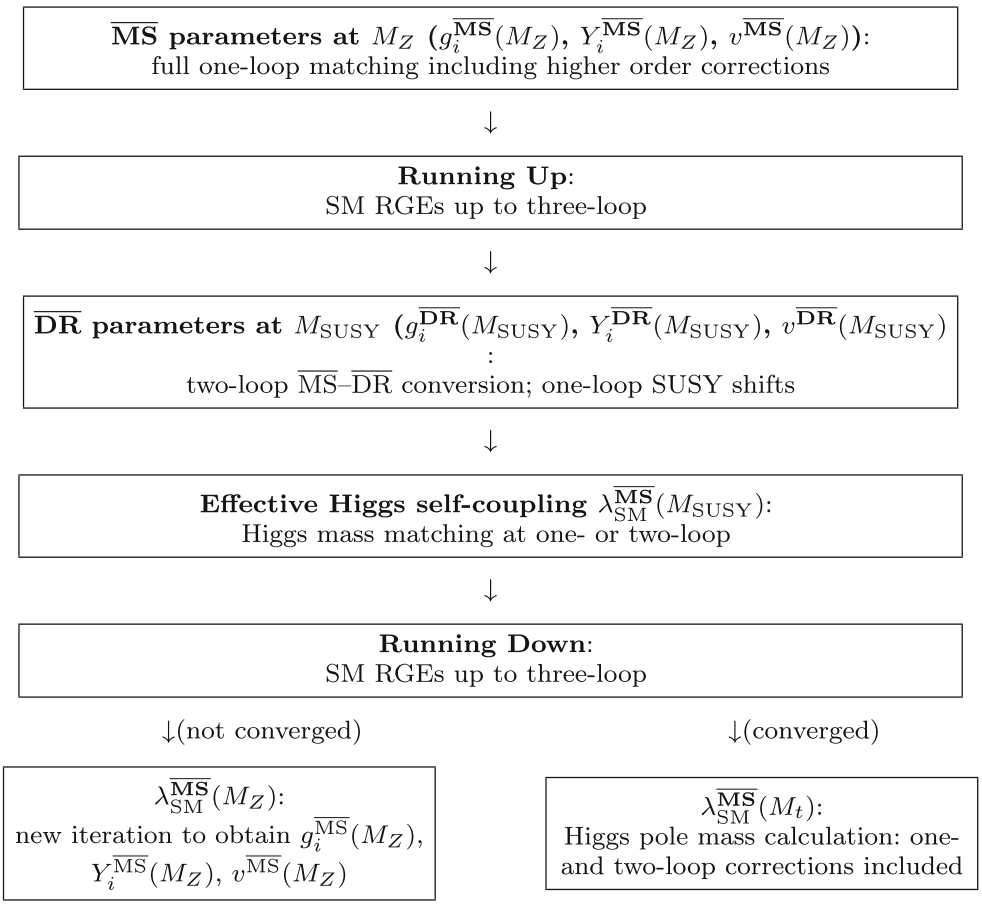

Fig. 1 Schematic procedure of the two-scale matching

matching agrees now rather well with the SoftSUSY results once the two-loop SUSY corrections in the matching are included up to several TeV. However, for even higher SUSY scales one finds that even the SUSY calculation with two-loop thresholds gives sizeable differences to the RGE re-summed calculation. On the other side, we find an excellent agreement with FlexibleSUSY, which performs also a two-scale matching but uses a different matching procedure at the SUSY scale.[2] A similar but less pronounced effect can be seen for the bottom Yukawa coupling. Here, the changes between the one- and two-scale matching account for a shift of about 6% for a SUSY scale of 100 TeV.

For the gauge couplings, the difference between the one- and two-scale matching are in general much smaller than for the Yukawa couplings. The changes are usually well below 1% even for a SUSY scale of 100 TeV. The only exception is SoftSUSY when turning on the two-loop thresholds to the strong coupling. In that case a significant decrease in g_3 with increasing M_{SUSY} is seen. This effect is not confirmed by the RGE re-summed calculations.

3.2 Gauge coupling unification

The shifts in the gauge couplings are rather small even for very large SUSY masses in the multi TeV range. Thus, they play phenomenologically only a sub-dominant role compared to the larger effects in the top Yukawa coupling. However, if one embeds the MSSM into a UV complete framework like supergravity, the running gauge couplings $g_1^{\overline{\text{DR}}}$ and $g_2^{\overline{\text{DR}}}$ are usually used as starting point to find the scale of grand unification, M_{GUT} by imposing the condition

$$g_1(M_{\text{GUT}}) = g_2(M_{\text{GUT}}). \tag{4}$$

Also the goodness of complete unification, i.e. the remaining difference between $g_3(M_{\text{GUT}})$ compared to the other two

[2] We have adapted the approach of Ref. [39] to a two-scale approach: we calculate the $\overline{\text{DR}}$ gauge and Yukawa couplings from the running $\overline{\text{MS}}$ values of α_{ew}, $\sin\Theta_W$, g_3 as well as from the running fermion masses and CKM matrix at the SUSY scale. The calculation is similar to the corresponding matching of the measured values of these parameters to the $\overline{\text{DR}}$ parameters at M_Z as before. All details are given in Appendix A.2. In contrast, FlexibleSUSY demands the equality of pole masses in the SM and MSSM at the SUSY scale to get the matching conditions for the SM gauge and Yukawa couplings.

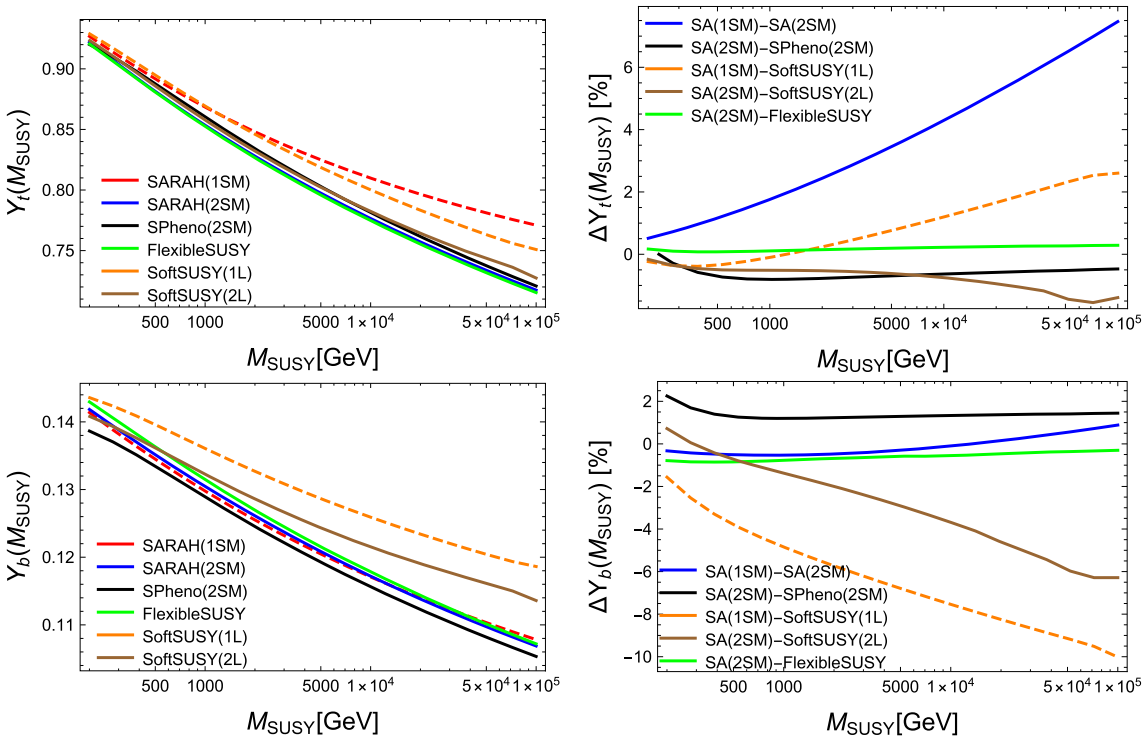

Fig. 2 The $\overline{\text{DR}}$ values of the running top and bottom Yukawa couplings at the SUSY scale. The *dashed red line* shows the result using the one-scale matching as done by earlier `SARAH/SPheno` version, while the *blue line* is the new results from `SARAH` and black the one from `SPheno`. In addition, we show the results for `SoftSUSY` using one-loop (*dashed orange*) and two-loop SUSY thresholds (*full brown*), as well as for `FlexibleSUSY` (*green*). On the right we give the difference $\Delta = \frac{Y^A - Y^B}{Y^A}$ between the results of two calculations as indicated

couplings is very sensitive to the values of $g_1^{\overline{\text{DR}}}$ and $g_2^{\overline{\text{DR}}}$ at M_{SUSY}. Therefore, we are checking the impact of the two-scale matching on M_{GUT} and $\Delta g = \frac{g_1(M_{\text{GUT}}) - g_3(M_{\text{GUT}})}{g_1(M_{\text{GUT}})}$ in a constrained version of the MSSM (CMSSM). The CMSSM has five input the parameters: the universal scalar mass m_0, the universal gaugino mass $M_{1/2}$, the universal trilinear soft-breaking parameter A_0, the ratio of the EW VEVs $\tan\beta = v_u/v_d$ and the phase of μ. All three dimensionful parameters, m_0, $M_{1/2}$ and A_0, are set at M_{GUT}. Here, we fixed

$$m_0 = M_{1/2}\,, \qquad \tan\beta = 10\,, \qquad A_0 = 0\,, \mu > 0, \tag{5}$$

and varied m_0 from 200 GeV up to 100 TeV. The results are shown in Fig. 4. The predicted value for the GUT scale as function of M_{SUSY} changes only slightly when using the new two-scale matching compared to the one-scale matching. In a complete GUT-model, the difference Δg has to be explained by threshold corrections to heavy GUT-scale particles [43,44] as we are using two-loop RGE running. Therefore, the right plot of this figure indicates the possible size of such corrections due to the GUT-scale spectrum. The prediction for Δg is different comparing the one- and two-scale matching, but also comparing the new results of `SARAH` and `SPheno`. The dominant origin of this difference is the inclusion of the two-loop correction to g_3 in `SPheno`, i.e. the difference between the two lines can be taken as an estimate for the theoretical uncertainty in Δg coming from higher order effects: only two-loop SM corrections in the matching of g_3 are included in `SPheno`, but not the two-loop SUSY thresholds. Also, for consistency three-loop RGEs of g_3 up to M_{GUT} would be necessary. However, for small m_0 also the terms $O(v^2/M_{\text{SUSY}}^2)$, which are neglected in `SPheno`, by computing the thresholds in the $SU(2)_L \times U(1)_Y$ limit become important and introduce a difference in the prediction of the GUT scale, which enters logarithmically in the unification condition.

3.3 SUSY masses

The changes in the $\overline{\text{DR}}$ parameters at the SUSY scale influence also the mass spectrum. This has very important consequences in particular on the Higgs mass which are discussed in the dedicated section Sect. 3.4. For now, we concentrate on the SUSY masses. In that case, the masses do hardly change if all SUSY specific parameters are defined at the SUSY scale

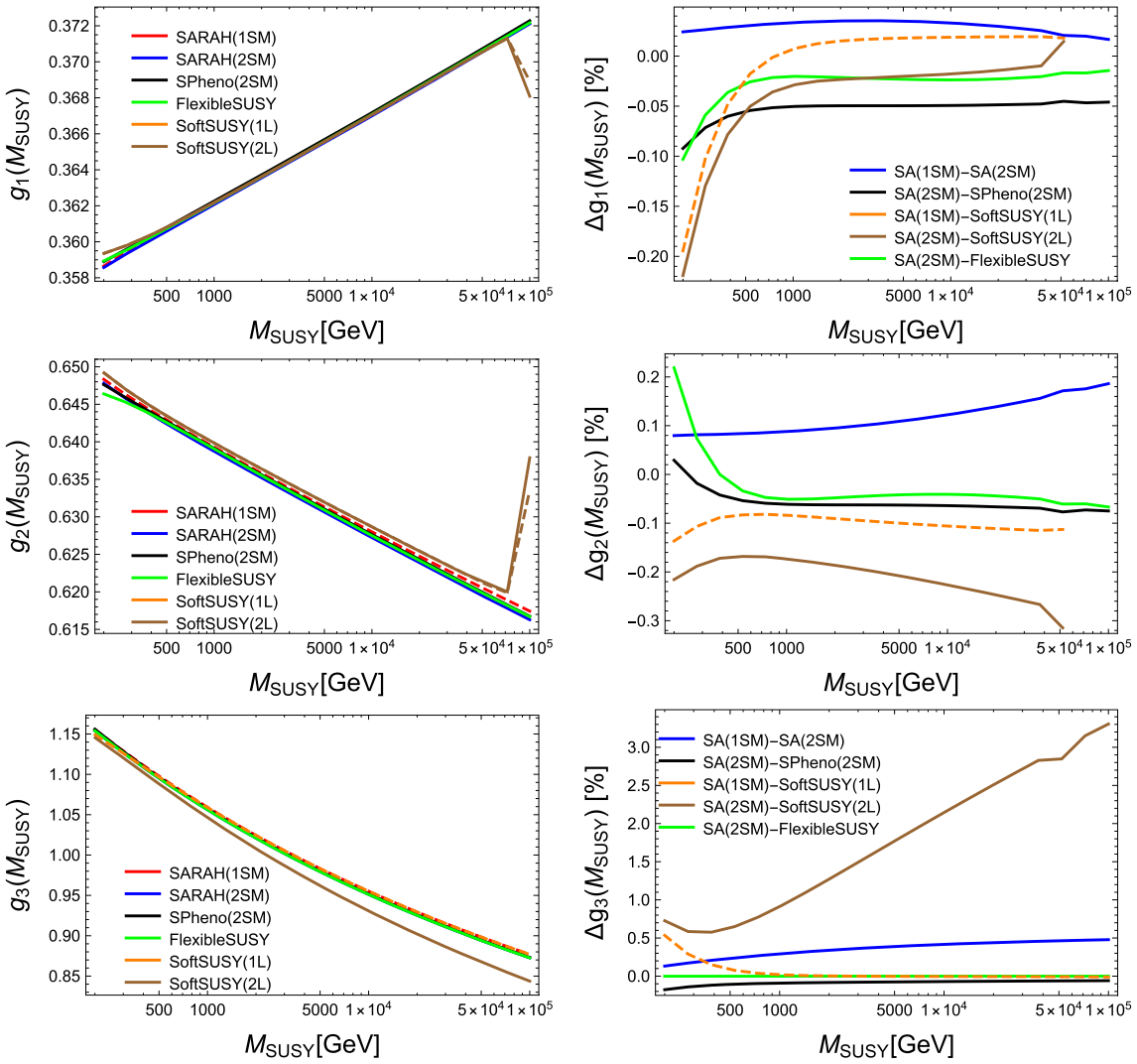

Fig. 3 The same as Fig. 2 for the gauge couplings g_1, g_2 and g_3

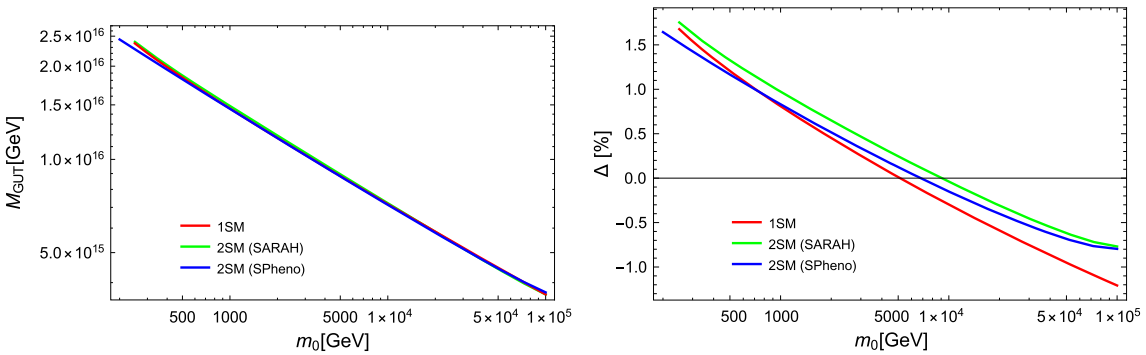

Fig. 4 On the *left*: the predicted value for $M_{\rm GUT}$ as a function of $m_0 = M_{1/2}$ in the CMSSM. The *red line* corresponds to the old one-scale matching, while the *blue* and *green line* are the results for the two-scale matching with `SARAH` and `SPheno`. On the *right*: the difference between $g_1(M_{\rm GUT})$ and $g_3(M_{\rm GUT})$ (in percent) as a function of m_0. The *colour code* is the same as on the *left*. We included here in `SPheno` the two-loop thresholds corrections to g_3

because only tiny changes in the F- and D-term contributions as well as in the radiative corrections will appear. Those are found to be hardly in the percent range even for large SUSY scales. Larger effects are present, if on considers unified scenarios in which the SUSY parameters are set via boundary conditions at a scale well above the SUSY scale. The additional RGE running between the high scale, which is often associated with the GUT scale via Eq. 4, will then introduce a larger dependence on $\overline{\text{DR}}$ values of SM gauge and Yukawa couplings at M_{SUSY}. As an example, we consider again the CMSSM. For simplicity, we fix in the following, if not stated otherwise, $A_0 = 0$, $\mu > 0$, $\tan\beta = 10$ and perform a scan over m_0 and $M_{1/2}$. The changes in the masses of the lightest stop, lightest stau, lightest neutralino and the gluino in the $(m_0, M_{1/2})$-plane are shown in Fig. 5. The largest effect in general can be seen for the light stop mass, which changes by 2–3% when pushing m_0 in the multi-TeV range. For the other masses, the changes in the $\overline{\text{DR}}$ parameters account only for moderate changes of 1% and below. The only exception are fine-tuned region with a higgsino LSP which we discuss below in more detail. Here, we also display the changes in the bino LSP mass because there small shifts can have sizeable effects in the calculation of the relic density, e.g. in the case of Higgs resonances or in the case of co-annihiliation.

The impact of the $\overline{\text{DR}}$ parameters at M_{SUSY} on the prediction of the light stop mass depends also on the chosen value for A_0. For non-vanishing A_0, the changes can become larger as shown in Fig. 6. Setting $A_0 = +1.5m_0$ we find that the stop mass changes by more than 5% for $m_0 > 4$ TeV. These changes are still very moderate and have hardly any phenomenological impact at the LHC. However, as mentioned above they can become important for instance in stau or stop co-annihilation to explain the dark matter abundance in the universe [45].

A much more pronounced effect can be observed for the μ parameter in the so called 'Focus-Point'-region [46–49]

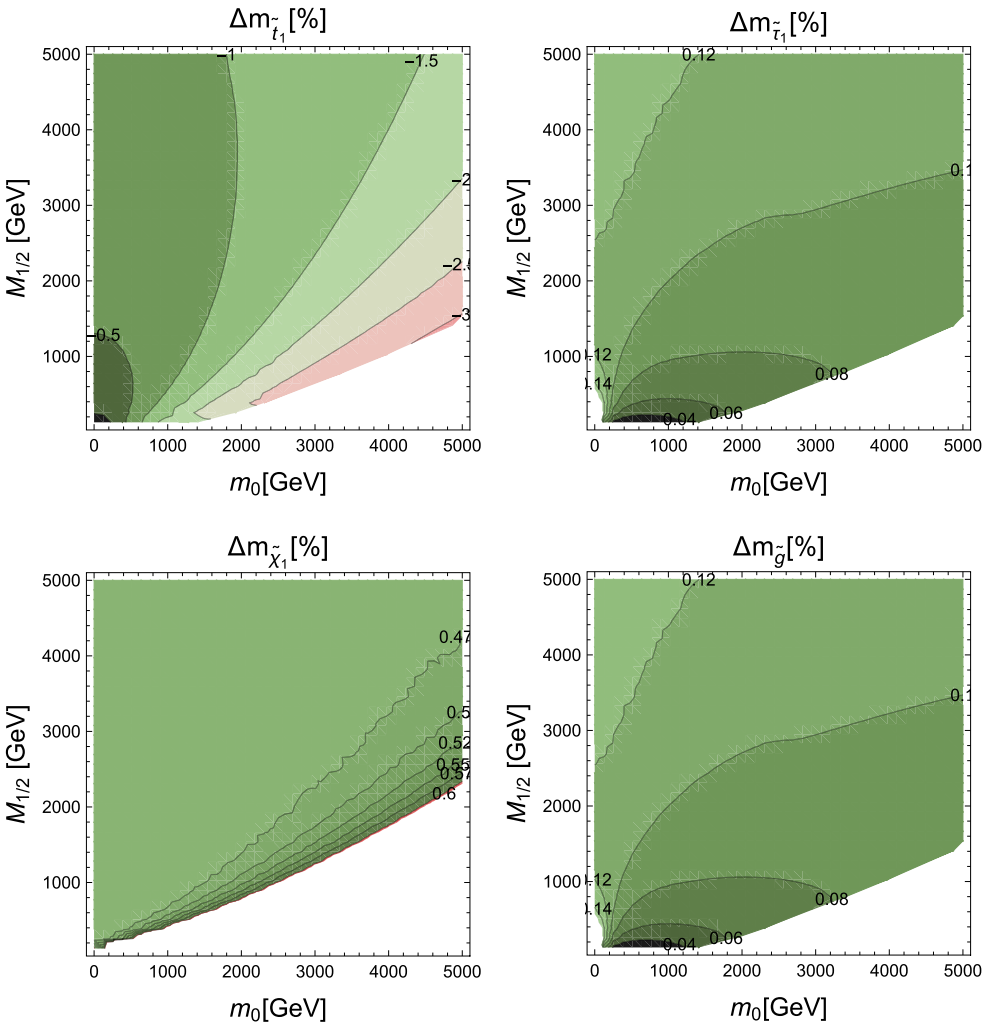

Fig. 5 The mass difference $\Delta = \frac{m^{\text{old}} - m^{\text{new}}}{m^{\text{old}}}$ in percent between the old and new mass calculation using SARAH. The *red* boundary in the $\tilde{\chi}_1^0$-plot shows the area with a higgsino LSP which is discussed in the text in more detail

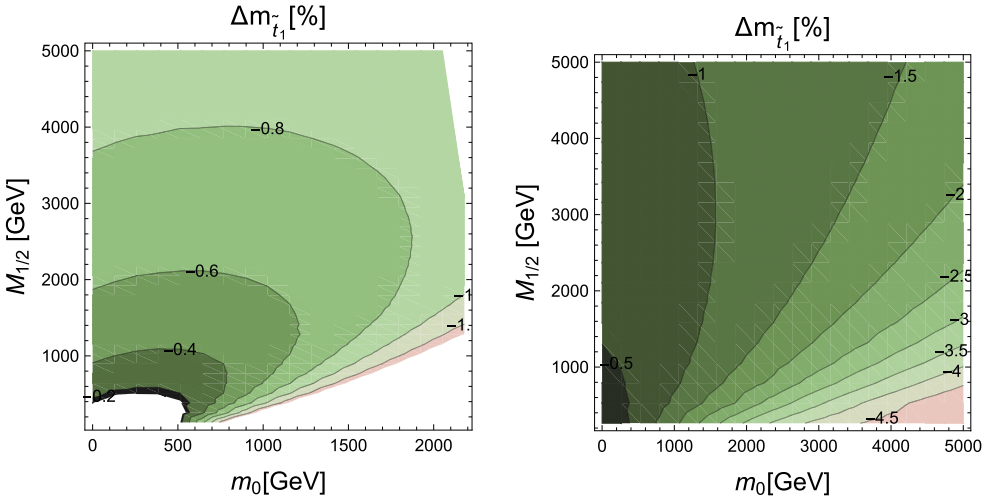

Fig. 6 The same as Fig. 5 for lightest stop but using $A_0 = -1.5m_0$ (*left*) and $A_0 = +1.5m_0$ (*right*)

from the minimisation conditions of the potential. This result at tree level in

$$|\mu|^2 = \frac{(m_{H_d}^2 - m_{H_u}^2 \tan\beta^2)}{\tan^2\beta - 1} - \frac{1}{2}M_Z^2 \simeq -m_{H_u}^2 - \frac{1}{2}M_Z^2 \tag{6}$$

where we have assumed in the last step $\tan\beta \gg 1$. The special feature of the focus point region is that cancellations in the RGE contributions to $m_{H_u}^2$ result in moderately small μ, which is much smaller than the other SUSY mass parameters. How well these cancellation work depends strongly on the value of the top Yukawa coupling. Hence, we find that in the focus point region, which is usually needs moderate $M_{1/2}$ and large m_0, the value of μ changes by more than 25% as shown in Fig. 7. Thus, also the higgsino masses vary significantly between the one- and two-scale matching calculation.

If one assumes that a large μ-parameter is the main source of fine-tuning in the MSSM, these changes in μ have also an impact on naturalness considerations. Using the approximate formula $\Delta \simeq \frac{\mu^2}{M_Z^2}$ as a measure for the fine-tuning,[3] one sees that the fine-tuning prediction could reduce a factor of 2 and more in the focus point region when going from the one-scale matching to the two-scale matching.

3.4 Higgs mass in the MSSM

The impact of heavy SUSY masses on the Higgs mass is nowadays a widely discussed topic. While fixed order calculations suffer from increasing uncertainties, there are two methods to improve the accuracy: (1) resumming the stop contributions as done by `FeynHiggs`; (2) working with a EFT ansatz as first done by `SusyHD` and later incorporated in `FlexibleSUSY` as well. The pole-mass matching described in Sect. 2, which was used so far only in `FlexibleSUSY` and now also by `SPheno/SARAH`, has the additional advantage that it includes terms $O(v^2/M_{\text{SUSY}}^2)$. This is in contrast to previous calculations to obtain λ_{SM} from the effective potential which are used by `SusyHD` for instance. Thus, these EFT calculation have a larger uncertainty for not too large M_{SUSY}, while the predictions using a pole-mass matching are still reliable for M_{SUSY} of 1 TeV and even below.

We give a comparison of the Higgs mass prediction of the new `SARAH` and `SPheno` versions against previous calculations as well as the current versions of `FeynHiggs` (2.12.2), `SusyHD` (1.0.2) and `FlexibleSUSY` (1.7.2).[4] For simplicity, we assume a degeneracy of the SUSY soft masses as well as M_A and μ at the SUSY scale:

$$M_1 = M_2 = M_3 = M_A = \mu \equiv M_{\text{SUSY}}, \tag{7}$$

$$m_{\tilde{e}}^2 = m_{\tilde{l}}^2 = m_{\tilde{d}}^2 = m_{\tilde{u}}^2 = m_{\tilde{q}}^2 = \mathbf{1}M_{\text{SUSY}}^2. \tag{8}$$

We neglect all trilinear soft-terms but the one involving the stops, which is parametrised as usual by

$$L = A_t Y_t \tilde{t}_L \tilde{t}_R^* H_u + \text{h.c.} \tag{9}$$

The results for the Higgs mass prediction for $A_t = 0, \pm M_{\text{SUSY}}$ and M_{SUSY} up to 100 TeV are summarised in Figs. 8, 9 and 10. One can see in Fig. 8 that the new calculation of `SPheno/SARAH` gives a significant lower Higgs mass

[3] These formula differs by a factor of 2 compared to the expression usually taken, $\Delta \simeq 2\frac{\mu^2}{M_Z^2}$, because of the incorporation of loop effects, which have been overlooked for a long time [50].

[4] We used for the following comparison the model file `MSSMtower` of `FlexibleSUSY` which also performs a pole-mass matching to get $\lambda_{\text{SM}}(M_{\text{SUSY}})$.

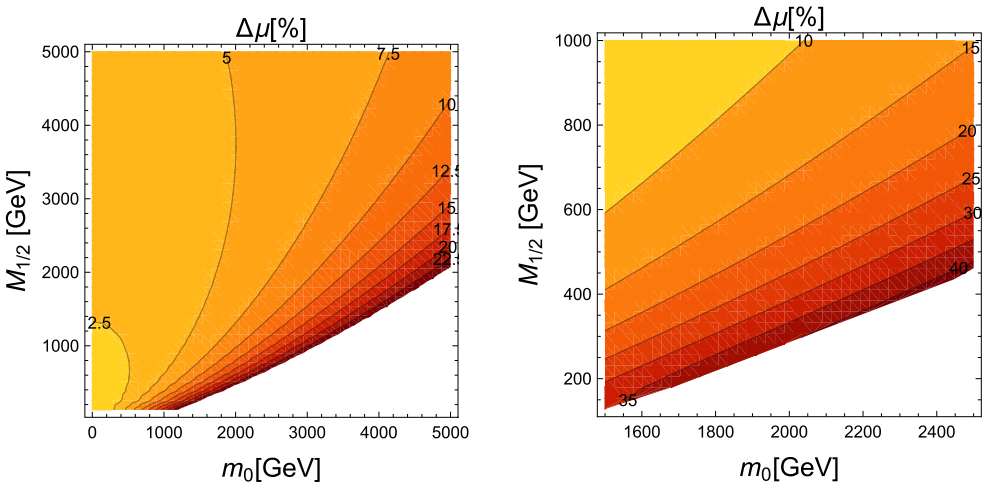

Fig. 7 The same as Fig. 5 for the value of μ at the SUSY scale. The *right* plot is a zoom into the interesting region of the *left one*

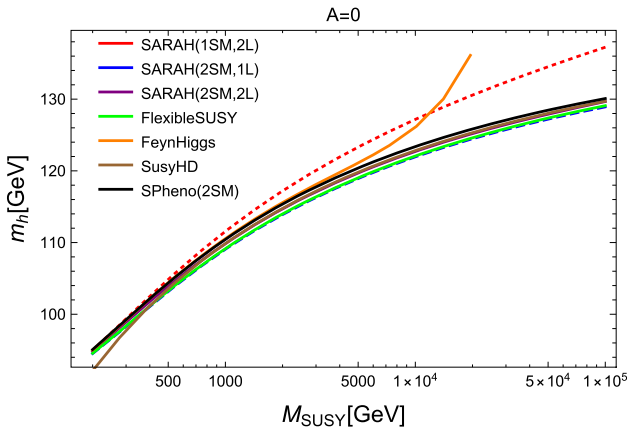

Fig. 8 The Higgs mass prediction of different computer codes as a function of the SUSY mass. The *dashed red line* corresponds to the old prediction by SARAH/SPheno

for very heavy SUSY scales and is in good agreement with the other codes like FlexibleSUSY and SusyHD for the entire range of $M_{\rm SUSY}$ shown here.[5] Only for small values of $M_{\rm SUSY}$ SusyHD deviates from the other codes because of terms $O(v^2/M^2_{\rm SUSY})$ missing due to the effective potential approach. The main reason for the large rise in the Higgs mass with SPheno/SARAH using a one-scale matching is the calculation of the top Yukawa coupling as discussed in Sect. 3.1. Since the calculation is not wrong per se, but the differences in the calculation of Y_t correspond to a three-loop effect in m_h, the large changes in the Higgs mass prediction show how large the theoretical uncertainty of the fixed order calculation can become for very large SUSY scales. It might be surprising that a formal three-loop effect has such a big impact. However, it was for instance discussed in Ref. [19] that at three-loop large cancellations appear, i.e. an incomplete three-loop calculation can give a quite misleading impression.

Since the agreement between the different codes becomes impressively good even for very large SUSY masses, we give in Fig. 9 the numerical differences between the Higgs mass predictions of SARAH compared to the other codes. Also the difference between the one-scale matching and the two-scale matching using a one- or two-loop calculation of λ is shown: for $M_{\rm SUSY} = 100$ TeV the Higgs mass prediction decreases by about 7 GeV when doing it via the EFT approach. The remaining difference from SusyHD and FlexibleSUSY is always better than 1 GeV, most often even better than 0.5 GeV.[6] The increasing difference between SARAH and FlexibleSUSY compared to SPheno and SusyHD comes from the calculation of the top Yukawa coupling in the SM: while SARAH and FlexibleSUSY use two-loop thresholds, SPheno and SusyHD have included even higher order corrections via the fit formula of Ref. [42]. These corrections need not to be included because they are of a higher loop level than the Higgs mass calculation is done. Thus, the difference between these two calculations give an impression of the minimal, theoretical uncertainty which is at least present. The differences between the codes also don't grow significantly if we use non-vanishing values for A_t as shown in Fig. 10: the overall changes in the Higgs mass between the SARAH calculation in the full MSSM and in the effective SM changes again by 7–8 GeV for very large

[5] The large rise in the Higgs mass as shown by FeynHiggs for $M_{\rm SUSY} > 5$ TeV stems from a conversion problem of the input parameters and will most likely disappear in the near future [51].

[6] The public version of FlexibleSUSY performs so far a one-loop matching for λ. We compare therefore the SARAH results of a two-loop matching only with FeynHiggs, SPheno and SusyHD, while we use for the comparison with FlexibleSUSY the one-loop matching results.

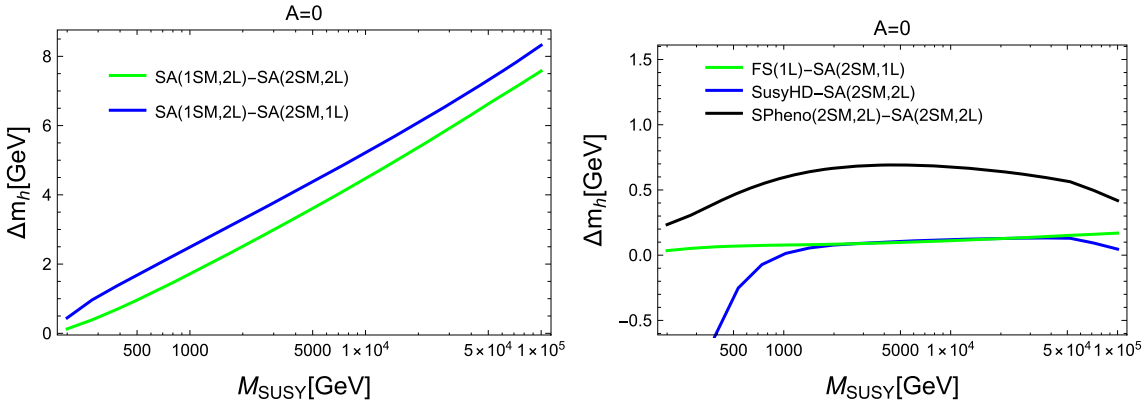

Fig. 9 On the *left*: difference between the Higgs mass as predicted by the new SARAH and the old version using one- (*blue*) or two-loop (*green*) matching conditions for λ_{SM} at the SUSY scale. On the *right*: the differences between SARAH and the new stand-alone SPheno version (*black*), SusyHD (*blue*; *dashed line* with three-loop thresholds to Y_t, full line without these corrections) as well as FlexibleSUSY. We used here vanishing trilinear soft-breaking stop couplings

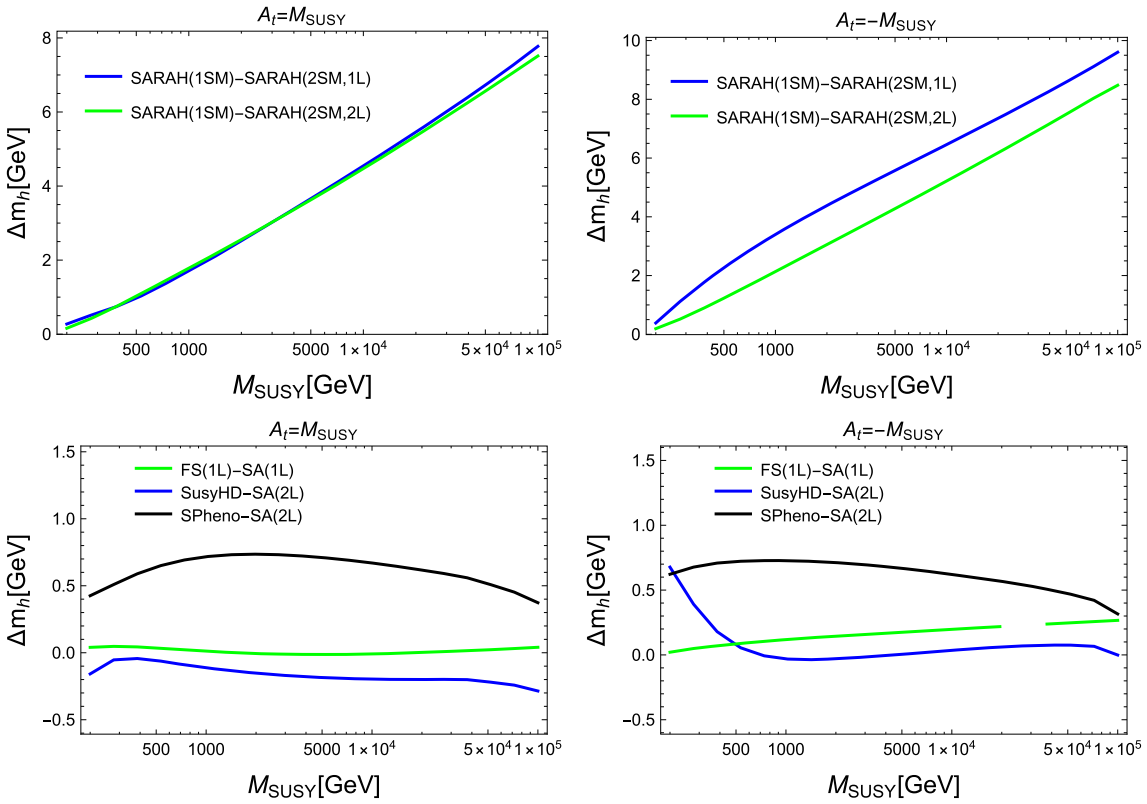

Fig. 10 The same as Fig. 9 for non-vanishing A_t

SUSY scales, while the difference from the other codes is in the range of 1 GeV and less.

3.5 Higgs mass beyond the MSSM

With SARAH it is also possible to generate a spectrum generator for models beyond the MSSM which calculates mass spectra, decays and precision observables [52]. Also for these models two-loop Higgs mass calculations are performed by default. All important two-loop corrections stemming from new particles and/or new interactions are covered as discussed in detail in Refs. [53–55]. The calculations make use of the generic results of Refs. [56–60] and the only approximations used in the SARAH implementation of the two-loop calculations are (1) the gaugeless limit, i.e. setting $g_1 = g_2 = 0$, and (2) neglecting the momentum

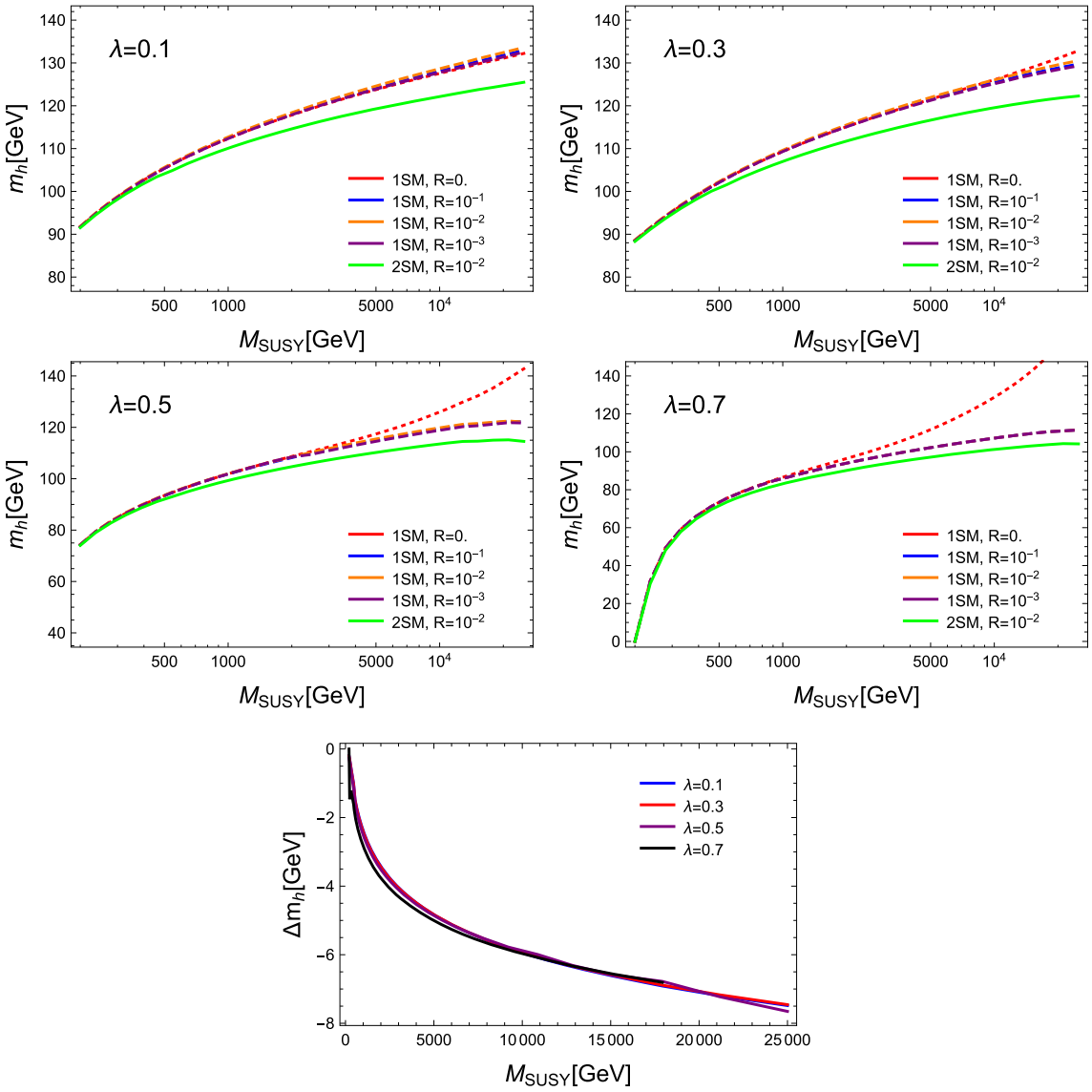

Fig. 11 The SM-like Higgs mass in the NMSSM as a function of the SUSY scale for four different values of λ (*first*, *second row*): the *dotted red line* gives the result of the one-scale matching (1SM) without regulator R, the *dashed lines* uses one-scale matching and $R = 10^{-1}, 10^{-2}, 10^{-3}$, while for the *green line* the two-scale matching (2SM) was used together with a Higgs mass calculation in the effective SM. The *third row* shows the difference Δm_h between the one-scale and two-scale matching (both with $R = 10^{-2}$)

dependence, i.e. $p^2 = 0$. Thus, SARAH provides for models beyond the MSSM the same precision in the Higgs mass as it does for the MSSM. Moreover, the obtained results with SARAH include already for the next-to-minimal supersymmetric standard model (NMSSM) corrections, which are not available otherwise [61,62]. However, there is one additional subtlety when using these two-loop corrections in extended Higgs sector which we need to discuss before coming to the results of the EFT approach: massless states appearing in the two-loop calculations usually cause divergences. Since the calculations are done in Landau gauge, these divergences are often associated with the Goldstone bosons of broken gauge groups which has motivated the name 'Goldstone boson catastrophe' [63,64]. For many cases this behaviour was already under control in SARAH by the treatment of the D-terms which induced finite Goldstone masses as explained in Ref. [55]. However, for large SUSY scales, it may still happen that the ratio m_S/M_{SUSY} for some scalar mass m_S becomes very small and introduces numerical problems. As short-term workaround we have introduced for this reason a regulator R which defines the minimal scalar mass squared as a function of the renormalisation scale Q,

$$m^2_{S,\min} = RQ^2. \tag{10}$$

All scalar masses which appear in the two-loop integrals which are smaller than $m^2_{S,\min}$ are then replaced by RQ^2. We found that the numerical dependence on R is usually small for values of R between 0.1 and 0.001. Nevertheless, the results of Ref. [65] shall be included in SARAH in the near future to have a rigorous solution to the Goldstone boson catastrophe which is independent of any regulator [66].

We can turn now to the discussion of the changes in the Higgs mass prediction when using the EFT ansatz. In general, it is possible to use the two-scale matching together with an effective calculation of the Higgs mass within the SM also for non-minimal models. The procedure is exactly the same as for the MSSM. SARAH uses the calculated Higgs mass in the full model to obtain $\lambda_{SM}(M_{SUSY})$ via a pole-mass matching. It then evaluates $\lambda_{SM}(m_t)$ and calculates m_h at that scale using SM corrections. We briefly discuss the impact of the new calculation at the example of the NMSSM.[7] For this purpose, we relate the NMSSM specific, dimensionful parameters to the SUSY scale via

$$\mu_{\text{eff}} = M_{SUSY}, \quad A_\kappa = -\lambda M_{SUSY}, \quad A_\lambda = M_{SUSY}\left(\frac{\tan\beta}{(1+\tan\beta^2)} - \frac{\kappa}{\lambda}\right).$$

With this parametrisation we find that the heavy MSSM-like scalars get a tree-level mass of M_{SUSY}, while also the scalar singlets are sufficiently heavy to be integrated out at M_{SUSY}. We set in addition

$$\tan\beta = 4, \quad \lambda = \kappa.$$

Thus, the only free parameters left are λ and M_{SUSY}. The Higgs mass for a variation of M_{SUSY} for $\lambda = 0.1, 0.3, 0.5, 0.7$ is shown in Fig. 11. Here, we also show the results with and without regulator R. One can see that the numerical problems associated with small masses, which in this case here are the light Higgs as well as the two Goldstone bosons, show up for increasing M_{SUSY}. The larger λ is, the more pronounced these problems are. However, with a regulator $R = 0.01$ this behaviour can be prevented for all values of λ and M_{SUSY} shown here for the one- and two-scale matching. We find that the results with regulator masses are in agreement with Ref. [12] within the indicated uncertainties.

The impact on the Higgs mass using the new two-scale matching is similar to the MSSM: for SUSY masses up to 2 TeV, the effects are small and less than 2 GeV, but they quickly increase with increasing M_{SUSY}. For $M_{SUSY} = 25$ TeV, the difference in the Higgs mass prediction is between 5.5 and 6.5 GeV. For our example we find that the differences depend only weakly on the value of λ.

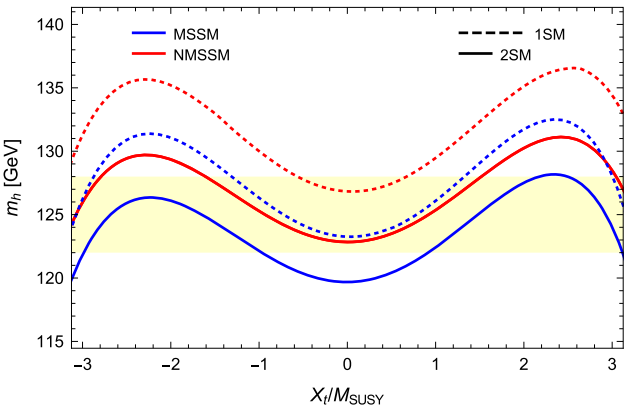

Fig. 12 The Higgs mass in the MSSM and NMSSM as a function of X_t/M_{SUSY} using one- and two-scale matching. Here we set $\mu = M_{SUSY} = 5$ TeV and used for the MSSM $\tan\beta = 10$, $M_A = 5$ TeV. The input parameters for the NMSSM were $\lambda = 0.6, \kappa = 0.2, A_\lambda = 10$ TeV, $A_\kappa = -5$ TeV, $\tan\beta = 2$

Similarly, one can now use SARAH to study also the Higgs masses for other models in the presence of large SUSY scales more precisely. However, a detailed exploration of these effects in other models is beyond the scope of this paper. Here, we want to stress that one should be careful with models with extended Higgs sector because not all scalar masses become automatically large if M_{SUSY} is large. Examples are for instance models with extended gauge sectors in which a second light scalar can appear because of D-flat directions [68–70]. In these cases, a sizeable mixing between the SM-like Higgs and another scalar can be present, i.e. the calculation of m_h within an effective SM might now be valid. Therefore, SARAH does not perform this calculation by default, if a second CP-even scalar with a mass below 500 GeV is present.

3.6 Perturbativity limit of new interactions

Many models beyond the MSSM are attractive because they give a tree-level enhancement of the Higgs mass. This is quite interesting from the point of view because it reduces the required loop contributions to obtain $m_h = 125.1$. Usually this allows for smaller values of A_t, which is important for the stability of the scalar potential [71–75]. The best studied example is again the NMSSM which pushes the Higgs mass via new F-term contributions which are proportional to λ^2. We demonstrate this in Fig. 13, where we compare the dependence of the Higgs mass on the stop mixing parameter X_t as defined as

$$X_t = A_t - \mu\tan\beta. \tag{11}$$

In the NMSSM, μ is replaced by μ_{eff}. We see for a SUSY scale of 5 TeV and the chosen value of $\tan\beta = 2$ and $\lambda = 0.6$

[7] We refer to Ref. [67] for an introduction into the NMSSM and for questions regarding the notation in the following.

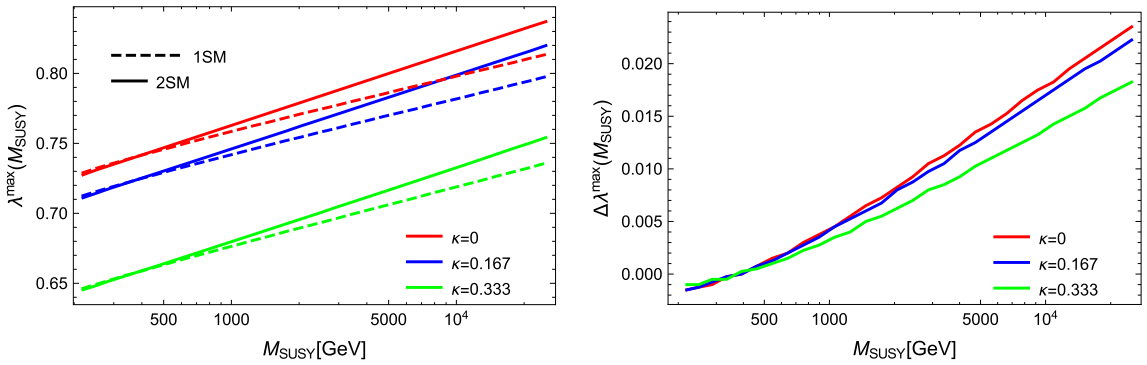

Fig. 13 *Left* maximal value of $\lambda(M_{\rm SUSY}$ consistent with perturbativity up to $M_{\rm GUT}$ for different values of κ. The *full* (*dashed*) *lines* correspond to the case of two- (one-) scale matching. *Right* the difference $\Delta\lambda = \lambda^{\rm max}_{\rm 2SM}(M_{\rm SUSY}) - \lambda^{\rm max}_{\rm 1SM}(M_{\rm SUSY})$ of the two matching schemes.

even without stop mixing the Higgs mass can be found in the correct mass range of 122–128 GeV (Fig. 12).

Because of this large impact of λ on the Higgs mass, it is very important to know how big λ can be in order to be still in agreement with gauge couplings unification at $M_{\rm GUT}$.

In Fig. 13 we display the maximal value of $\lambda(M_{\rm SUSY})$, which does not lead to a Landau pole below $M_{\rm GUT}$ for different values of $\kappa(M_{\rm SUSY})$ and for $M_{\rm SUSY}$ up to 25 TeV and $\tan\beta = 4$, and show the differences between the one- and two-scale matching. Because of the smaller top Yukawa coupling in the two-scale approach, one finds that slightly larger values of $\lambda(M_{\rm SUSY}$ are allowed than for the one-scale matching.

4 Conclusion

We have presented the new two-scale matching procedure in SARAH/SPheno to improve the prediction of the running $\overline{\rm DR}$ gauge and Yukawa couplings at the SUSY scale for large values of $M_{\rm SUSY}$. Together with the new matching, also the possibility of an EFT Higgs mass calculation is introduced. In the EFT calculation λ_{SM} is obtained via a Higgs pole-mass matching at $M_{\rm SUSY}$ and the SM-like Higgs mass is calculated within the SM at the top mass scale. We have shown various consequences of the two-scale matching and the EFT Higgs mass calculation in the MSSM and beyond. In particular, we have compared the Higgs mass prediction for SUSY scales up to 100 TeV and found good agreement with other EFT codes as SusyHD and FlexibleSUSY. We have also shown that the value of μ in the CMSSM can change significantly because of the changes in the top Yukawa coupling. This has a direct impact on naturalness considerations.

Acknowledgements We thank Alexander Voigt for helpful discussions concerning the matching procedure in FlexibleSUSY and Eliel Camargo for his contribution in the early stage of this work. W.P. has been supported by the DFG, project nr. PO 1337/7-1.

Appendix A Matching

Appendix A.1 One-scale matching

Before we present the new two-scale matching which is now performed by SARAH/SPheno, we review the current procedure. The first step is that all $\overline{\rm DR}$ parameters are calculated already at m_Z and two-loop SUSY RGEs are used for the running to $M_{\rm SUSY}$.

Appendix A.1.1 Strong coupling

The strong interaction coupling at the weak scale is matched to the input value $\alpha_s^{(5)}(m_Z)$ in the $N_f = 5$ flavour scheme via

$$\alpha_s^{\overline{\rm DR}}(m_Z) = \frac{\alpha_s^{(5),\overline{\rm MS}}(m_Z)}{1 - \Delta\alpha_s(m_Z)}, \tag{A.1}$$

$$\Delta\alpha_s(m_Z) = \frac{\alpha_s}{2\pi}\left(\frac{1}{2} - \frac{2}{3}\log\frac{m_t}{m_Z} + \Delta_s^{\rm MSSM}\right). \tag{A.2}$$

The corrections due to the new coloured states in the MSSM are given by

$$\Delta_s^{\rm MSSM} = -2\log\frac{m_{\tilde g}}{m_Z} - \frac{1}{6}\sum_{i=1}^{6}\left(\log\frac{m_{\tilde u_i}}{m_Z} + \log\frac{m_{\tilde d_i}}{m_Z}\right). \tag{A.3}$$

For any other BSM model, $\Delta_s^{\rm MSSM}$ is adjusted by SARAH to fit to the particle content.

Appendix A.1.2 Electroweak sector

The EW gauge sector of the MSSM is determined by four fundamental parameters. These are usually the gauge couplings for $SU(2)_L \times U(1)_Y$ and the electroweak VEVs for the up- and down-Higgs

$$g_1, \quad g_2, \quad v_d, \quad v_u;$$

v_d and v_u are derived from the calculated EW VEV $v(m_Z)^2 = \sqrt{v_d^2 + v_u^2}$ and the input value for $\tan\beta = \frac{v_u}{v_d}$, which could either be given at m_Z or $M_{\rm SUSY}$. Thus, the matching procedure needs to determinate $v^{\overline{\rm DR}}(m_Z)$, $g_1^{\overline{\rm DR}}(m_Z)$ and $g_2^{\overline{\rm DR}}(m_Z)$ from three physical quantities. Here, SPheno and SARAH use as input the Z mass, the Fermi constant G_F and the electromagnetic coupling of the SM at the scale m_Z in the 5-flavour scheme, $\alpha_{em}^{(5),\overline{\rm MS}}(m_Z)$.

The relations between the input and $\overline{\rm DR}$ parameters is as follows:

1. The electroweak coupling constant is calculated from

$$\alpha_{em}^{\overline{\rm DR}}(m_Z) = \frac{\alpha_{em}^{(5),\overline{\rm MS}}(m_Z)}{1 - \Delta\alpha(m_Z)}, \tag{A.4}$$

$$\Delta\alpha(m_Z) = \frac{\alpha}{2\pi}\left(\frac{1}{3} - \frac{16}{9}\log\frac{m_t}{m_Z} + \Delta_{em}^{\rm MSSM}\right). \tag{A.5}$$

with

$$\Delta_{em}^{\rm MSSM} = -\frac{4}{9}\sum_{i=1}^{6}\log\frac{m_{\tilde{u}_i}}{m_Z} - \frac{1}{9}\sum_{i=1}^{6}\log\frac{m_{\tilde{d}_i}}{m_Z} - \frac{4}{3}\sum_{i=1}^{2}\log\frac{m_{\tilde{\chi}_i^+}}{m_Z} - \frac{1}{3}\sum_{i=1}^{6}\log\frac{m_{\tilde{e}_i}}{m_Z} - \frac{1}{3}\log\frac{m_{H^+}}{m_Z} \tag{A.6}$$

Again, if another model shall be considered, the value of Δ_{em} is calculated by SARAH automatically.

2. The Weinberg angle $\sin^{\overline{\rm DR}}\Theta_W$ at the scale m_Z is obtained iteratively from the above-computed $\alpha_{em}^{\overline{\rm DR}}(m_Z)$, together with G_F and m_Z, via

$$\left(\sin^{\overline{\rm DR}}\Theta_W \cos^{\overline{\rm DR}}\Theta_W\right)^2 = \frac{\pi\,\alpha_{em}^{\overline{\rm DR}}(m_Z)}{\sqrt{2} m_Z^2 G_F (1 - \delta_r)}, \tag{A.7}$$

where we have introduced

$$\delta_r = \hat{\rho}\frac{\Pi_{WW}^T(0)}{M_W^2} - \frac{\Re{\rm e}\Pi_{ZZ}^T(m_Z^2)}{m_Z^2} + \delta_{\rm VB} + \delta_r^{(2)}, \tag{A.8}$$

$$\hat{\rho} = \frac{1}{1 - \Delta\hat{\rho}}, \quad \Delta\hat{\rho} = \Re{\rm e}\left[\frac{\Pi_{ZZ}^T(m_Z^2)}{\hat{\rho}\, m_Z^2} - \frac{\Pi_{WW}^T(M_W^2)}{M_W^2}\right] + \Delta\hat{\rho}^{(2)}. \tag{A.9}$$

Here, $\Pi_{VV}^T(p^2)$ $(V = Z, W)$ are the $\overline{\rm DR}$-renormalized transverse parts of the self-energies of the vector bosons, computed at the renormalisation scale $Q = m_Z$, and $\delta_r^{(2)}$ and $\Delta\hat{\rho}^{(2)}$ are two-loop corrections as given in [39,76],

$$\delta_r^{(2)} = \frac{f_1}{(1 - \sin^2\Theta_W^{\overline{\rm MS}})\sin^2\Theta_W^{\overline{\rm MS}}} - x_t(1 - \delta_r)\rho \tag{A.10}$$

with

$$x_t = 3\left(\frac{G_F m_t^2}{8\pi^2}\right)^2 \rho_2\left(\frac{m_h}{m_t}\right), \tag{A.11}$$

$$f_1 = \frac{\alpha_S^{\overline{\rm MS}}\alpha_{ew}^{\overline{\rm MS}}}{4\pi^2}\left(2.145\frac{m_t^2}{m_Z^2} + 0.575\log\frac{m_t}{m_Z} - 0.224 - 0.144\frac{m_Z^2}{m_t^2}\right), \tag{A.12}$$

$$f_2 = \frac{\alpha_S^{\overline{\rm MS}}\alpha_{ew}^{\overline{\rm MS}}}{4\pi^2}\left(-2.145\frac{m_t^2}{m_Z^2} + 1.262\log\frac{m_t}{m_Z} - 2.24 - 0.85\frac{m_Z^2}{m_t^2}\right), \tag{A.13}$$

and

$$\rho_2(r) = 19 - 16.5r + \frac{43}{12}r^2 + \frac{7}{120}r^3 - \pi\sqrt{r}\left(4 - 1.5r + \frac{3}{32}r^2 + \frac{r^3}{256}\right) - \pi^2(2 - 2r + 0.5r^2) - \log(r)(3r - 0.5r^2). \tag{A.14}$$

The one-loop vertex and box corrections $\delta_{\rm VB}$ implemented into SPheno are hard-coded and taken from literature[77–79], while the ones used by SARAH are auto-generated and include therefore all one-loop corrections beyond the MSSM. Also the self-energies Π^T are automatically calculated by SARAH at the full one-loop level.

3. The electroweak VEV v used to calculate v_d and v_u at m_Z is obtained from

$$v^{\overline{\rm DR}}(m_Z) = \sqrt{m_Z^{\overline{\rm DR}}(m_Z)^2 \, \frac{(1-\sin^2\Theta_W^{\overline{\rm DR}})\sin^2\Theta_W^{\overline{\rm DR}}}{\pi\alpha^{\overline{\rm DR}}}}. \tag{A.15}$$

Here, the running mass $m_Z^{\overline{\rm DR}}$ is given by

$$M_Z^{\overline{\rm DR}}(M)Z) = \sqrt{m_Z^2 + \Pi_{ZZ}^T(m_Z^2)}. \tag{A.16}$$

Appendix A.1.3 Yukawa couplings

In order to calculate the value of the $\overline{\rm DR}$-renormalized Yukawa coupling at the SUSY scale, `SPheno` used so far the approach of Ref. [39]. First, for all leptons and the five light quarks the $\overline{\rm DR}$ masses at m_Z are calculated. Afterwards, the additional non-SUSY thresholds stemming from massive bosons and the full one-loop SUSY thresholds are included. For m_t also the known two-loop QCD corrections are added [80,81]

$$\Sigma_{\rm QCD}^{(2)} = \frac{1}{16\pi^2}\alpha_s 18\left(2011 - 1476\log(Q) + 396(\log(Q))^2 - 48\zeta_3 + 16\pi^2(1+2\log 2)\right). \tag{A.17}$$

Using these loop corrections, the loop-corrected 3×3 mass matrices for quarks and leptons are calculated via

$$m_f^{(1L)}(p_i^2) = m_f^{(T)} - \Sigma_{S,f}(p_i^2) - \Sigma_{R,f}(p_i^2)m_f^{(T)} - m_f^{(T)}\Sigma_{L,f}(p_i^2) \tag{A.18}$$

with $f = l, d, u$. Here, $\Sigma_{S,R,L}$ are usually the one-loop self-energies *without* photon and gluon corrections. Only for the top-quark, photon and gluon corrections need to be included and in addition one identifies

$$\Sigma_{S,t} = \Sigma_{S,t}^{(1)} + \Sigma_{QCD}^{(2)}. \tag{A.19}$$

The $\overline{\rm DR}$ Yukawa matrices fulfilling

$$m_u^{(T)} = \frac{1}{\sqrt{2}}Y_u v_u, \quad m_d^{(T)} = \frac{1}{\sqrt{2}}Y_d v_d, \quad m_l^{(T)} = \frac{1}{\sqrt{2}}Y_l v_l, \tag{A.20}$$

are calculated iteratively from Eq. (A.46) by the condition that the eigenvalues of $m_f^{(1L)}(p_i^2)$ must coincide with the $\overline{\rm DR}$ values for the light leptons and the top pole mass, respectively.

Appendix A.2 Two-scale matching

In the new two-scale approach, the separation of the matching is that all SM corrections are included at m_Z to obtain the $\overline{\rm MS}$ values which are then shifted at $M_{\rm SUSY}$ to their $\overline{\rm DR}$ values by including all one-loop SUSY thresholds.

Appendix A.2.1 Calculating the $\overline{MS}$ parameters at m_Z

The calculation of the $\overline{\rm MS}$ parameters at m_Z is very similar to the approach described in the last section, but with all BSM contributions removed.

1. We get for the gauge couplings

$$\alpha_S^{\overline{\rm MS}} = \frac{\alpha_s^{(5),\overline{\rm MS}}(m_Z)}{1+\frac{2}{3}\frac{\alpha_s}{2\pi}\left(\log\frac{m_t}{m_Z}\right)}, \tag{A.21}$$

$$\alpha_{ew}^{\overline{\rm MS}} = \frac{\alpha_{em}^{(5),\overline{\rm MS}}(m_Z)}{1+\frac{\alpha}{2\pi}\left(\frac{16}{9}\log\frac{m_t}{m_Z}\right)}. \tag{A.22}$$

2. The Weinberg angle is calculated as

$$\sin\Theta_W^{\overline{\rm MS}} = \frac{1}{2} - \sqrt{\frac{1}{4} - \frac{\pi\alpha_{ew}^{\overline{\rm MS}}(m_Z)}{\sqrt{2}m_Z^2 G_F(1-\delta_r)}} \tag{A.23}$$

with δ_r defined in Eq. (A.8). The following one-loop SM contributions are used:

$$\delta_{VB} = g_2^{\overline{\rm MS},2}\rho\left(6 + \frac{\log\cos^2\Theta_W}{\sin^2\Theta_W}\left(\frac{7}{2} - \frac{5}{2}\sin^2\Theta_W - \sin^2\Theta_W^{\overline{\rm MS}}\left(5 + \frac{3}{2}\frac{\cos^2\Theta_W}{\cos^2\Theta_W^{\overline{\rm MS}}}\right)\right)\right), \tag{A.24}$$

and the two-loop corrections $\delta_r^{(2)}$ agree with the ones used in the one-scale matching.

3. The VEV is obtained from

$$v^{\overline{\rm MS}} = (m_Z^{2,\overline{\rm MS}}(M_{\rm mZ}) + \delta m_Z^{2,\overline{\rm MS}})\frac{(1-\sin\Theta_W^{\overline{\rm MS}})\sin\Theta_W^{\overline{\rm MS}}}{\pi\alpha_{ew}^{\overline{\rm MS}}(M_{\rm mZ})} \tag{A.25}$$

where $\delta m_Z = \Pi_{ZZ}^T(m_Z^2)$ includes only the SM corrections.

4. The Yukawa couplings are obtained from the running $\overline{\rm MS}$ quark and lepton masses. Here, we include for m_t the

two-loop corrections to relate the $\overline{\rm MS}$ and pole mass[82]

$$m_t^{\overline{\rm MS}} = m_t^{\rm pole}\Big[1 + \frac{1}{16\pi^2}\left(\left(\frac{16\pi}{9}\alpha - \frac{16\pi}{3}\alpha_s\right)(4+\log(Q))\right) - \frac{1}{(16\pi^2)}\frac{\alpha_s^2}{18}(2821 + 2028\log(Q) + 396(\log(Q))^2 + 16\pi^2(1+2\log 2) - 48\zeta_3)\Big]. \tag{A.26}$$

The $\overline{\rm MS}$ Yukawa matrices are calculated iteratively from the condition that the $\overline{\rm MS}$ fermion masses are reproduced once the one-loop SM corrections with massive bosons are included:

$$m_f^{(1L)}(p_i^2) = m_f^{(T)} - \tilde{\Sigma}_S(p_i^2) - \tilde{\Sigma}_R(p_i^2)m_f^{(T)} - m_f^{(T)}\tilde{\Sigma}_L(p_i^2). \tag{A.27}$$

Here, $\tilde{\Sigma}$ are the self-energies without the photonic and gluonic contributions. The eigenvalues of $m_f^{(1L)}(p_i^2)$ must coincide with $m_f^{\overline{\rm MS}}(m_Z)$.

$g_i^{\overline{\rm MS}}$ $(i = 1,2,3)$, $Y_f^{\overline{\rm MS}}$ $(f = l,d,u)$ and $v^{\overline{\rm MS}}$ are then evaluated from m_Z to $M_{\rm SUSY}$ using the full two-loop SM RGEs which are extended by the three-loop contributions involving g_3, λ and Y_t.

For the top Yukawa and strong gauge coupling one can include in `SPheno` an additional threshold at m_t at which higher order corrections are included by using the fit formulae [42]

$$Y_t(m_t) = 0.9369 + 0.00556\left(\frac{m_t}{GeV} - 173.34\right) - 0.6(\alpha_s(m_Z) - 0.1184), \tag{A.28}$$

$$g_3(m_t) = 1.1666 + 0.00314\frac{(\alpha_s(m_Z) - 0.1184)}{0.0007} - 0.00046\left(\frac{m_t}{GeV} - 173.34\right). \tag{A.29}$$

Appendix A.2.2 Calculating the $\overline{DR}$ parameters at M_{SUSY} in `SARAH`

At the $M_{\rm SUSY}$, the $\overline{\rm MS}$ parameters are first shifted to $\overline{\rm DR}$ parameters and then the SUSY thresholds are added.

1. **Strong coupling**

$$\alpha_S^{\overline{\rm DR}}(M_{\rm SUSY}) = \frac{\alpha_S^{\overline{\rm MS}}(M_{\rm SUSY})}{1 - \Delta_{\alpha_S}^{\overline{\rm DR}}} \tag{A.30}$$

with

$$\Delta_{\alpha_S}^{\overline{\rm DR}} = \frac{\alpha_s}{2\pi}\left(\frac{1}{2} - \Delta_s^{\rm MSSM}\right). \tag{A.31}$$

2. **Electroweak sector**:
The electroweak gauge coupling is calculated from $g_1^{\overline{\rm MS}}$, $g_2^{\overline{\rm MS}}$ and translated into its $\overline{\rm DR}$ value via

$$\alpha_{ew}^{\overline{\rm MS}}(M_{\rm SUSY}) = \frac{1}{4\pi}\frac{(g_1^{\overline{\rm MS}}g_2^{\overline{\rm MS}})^2}{(g_1^{\overline{\rm MS}})^2 + (g_2^{\overline{\rm MS}})^2}, \tag{A.32}$$

$$\alpha_{ew}^{\overline{\rm DR}}(M_{\rm SUSY}) = \frac{\alpha_{ew}^{\overline{\rm MS}}(M_{\rm SUSY})}{1 - \Delta^{\overline{\rm DR}}}, \tag{A.33}$$

with

$$\Delta^{\overline{\rm DR}} = \frac{\alpha_{ew}^{\overline{\rm DR}}}{2\pi}\left(\frac{1}{3} + \Delta_{em}^{\rm MSSM}\right) \tag{A.34}$$

where m_Z has to be replaced by $M_{\rm SUSY}$ in Eq. (A.6). In addition, it is helpful to define for later use

$$\sin\Theta_W^{\overline{\rm MS}} = \frac{g_1^{\overline{\rm MS}}}{\sqrt{(g_1^{\overline{\rm MS}})^2 + (g_2^{\overline{\rm MS}})^2)}}, \tag{A.35}$$

$$\delta_r^{\overline{\rm MS}} = 1 - \frac{\pi\alpha_{ew}^{\overline{\rm MS}}(M_{\rm SUSY})}{\sqrt{2}G_F m_Z^2 \sin^2\Theta_W^{\overline{\rm MS}}(1 - \sin^2\Theta_W^{\overline{\rm MS}})}, \tag{A.36}$$

as well as

$$\delta_{VB}^{\overline{\rm DR}} = \delta_{VB}^{\rm MSSM} - \delta_{VB}^{\rm SM}, \tag{A.37}$$

$$\delta m_Z^{2,\overline{\rm DR}} = \Pi_{ZZ}^{T,\rm MSSM} - \Pi_{ZZ}^{T,\rm SM}, \tag{A.38}$$

$$\delta W_Z^{2,\overline{\rm DR}} = \Pi_{WW}^{T,\rm MSSM} - \Pi_{WW}^{T,\rm SM}. \tag{A.39}$$

Here $\Pi_{WW}^{T,\rm MSSM}$ are the full one-loop self-energies within the MSSM. Therefore, one needs to subtract $\Pi_{VV}^{T,\rm SM}$ to include only the new physics contributions. Thus, for consistency, one needs to evaluate here $\Pi_{ZZ}^{T,\rm SM}$ in the $\overline{\rm DR}$ scheme.

The $\overline{\rm DR}$ values of the Weinberg angle and electroweak VEV are now given by

$$\sin^2\Theta_W^{\overline{\rm DR}} = \frac{1}{2} - \sqrt{\frac{1}{4} - \frac{\pi\alpha_{ew}^{\overline{\rm DR}}(M_{\rm SUSY})}{\sqrt{2}m_Z^2 G_F(1 - \delta_r^{\overline{\rm MS}} - \delta_r)}}, \tag{A.40}$$

$$v^{\overline{\rm DR}} = \left(m_Z^{2,\overline{\rm MS}}(M_{\rm SUSY}) + \delta m_Z^{2,\overline{\rm DR}}\right)$$

$$\frac{(1-\sin\Theta_W^{\overline{\rm DR}})\sin\Theta_W^{\overline{\rm DR}}}{\pi\alpha_{ew}^{\overline{\rm DR}}(M_{\rm SUSY})}, \tag{A.41}$$

where the SUSY corrections are calculated as

$$\delta_r = \frac{1+\delta m_Z^{2,\overline{\rm DR}}/m_Z^2}{1+\delta W_Z^{2,\overline{\rm DR}}/m_W^2}\frac{\delta W_Z^{2,\overline{\rm DR}}}{m_W^2} - \frac{\delta m_Z^{2,\overline{\rm DR}}}{m_Z^2} + \delta_{VB}^{\overline{\rm DR}}. \tag{A.42}$$

$\sin\Theta_W^{\overline{\rm DR}}$ and $v^{\overline{\rm DR}}$ together with the calculated $\alpha_{ew}^{\overline{\rm DR}}(M_{\rm SUSY})$ and the input value for $\tan\beta$ determines $g_1^{\overline{\rm DR}}(M_{\rm SUSY})$, $g_2^{\overline{\rm DR}}(M_{\rm SUSY})$, $v_d^{\overline{\rm DR}}(M_{\rm SUSY})$, $v_u^{\overline{\rm DR}}(M_{\rm SUSY})$.

3. **Yukawa couplings** As a first step, the running $\overline{\rm MS}$ Yukawa couplings are translated in $\overline{\rm DR}$ values via [83]

$$m_{e,\mu,\tau}^{\overline{\rm DR}}(M_{\rm SUSY}) = m_{e,\mu,\tau}^{\overline{\rm MS}}(M_{\rm SUSY})\times\left(1-\frac{\alpha_{\rm EW}^{\overline{\rm DR}}}{4\pi}\right), \tag{A.43}$$

$$m_{d,s,b}^{\overline{\rm DR}}(M_{\rm SUSY}) = m_{d,s,b}^{\overline{\rm MS}}(M_{\rm SUSY}) \times\left(1-\frac{\alpha_S^{\overline{\rm DR}}}{3\pi}-\frac{43(\alpha_S^{\overline{\rm DR}})^2}{144\pi^2}-\frac{\alpha_{\rm EW}^{\overline{\rm DR}}}{4\pi}\frac{1}{9}\right), \tag{A.44}$$

$$m_{u,c,t}^{\overline{\rm DR}}(M_{\rm SUSY}) = m_{u,c,t}^{\overline{\rm MS}}(M_{\rm SUSY}) \times\left(1-\frac{\alpha_S^{\overline{\rm DR}}}{3\pi}-\frac{43(\alpha_S^{\overline{\rm DR}})^2}{144\pi^2}-\frac{\alpha_{\rm EW}^{\overline{\rm DR}}}{4\pi}\frac{4}{9}\right). \tag{A.45}$$

The running Yukawa couplings are obtained from

$$m_f^{(1L)}(p_i^2) = m_f^{(T)} - \tilde{\Sigma}_S(p_i^2) - \tilde{\Sigma}_R(p_i^2)m_f^{(T)} - m_f^{(T)}\tilde{\Sigma}_L(p_i^2). \tag{A.46}$$

Here, $\tilde{\Sigma}$ are the self-energies without SM contributions. The eigenvalues of $m_f^{(1L)}(p_i^2)$ must coincide with $m_f^{\overline{\rm DR}}(M_{\rm SUSY})$.

Appendix A.2.3 Calculating the $\overline{DR}$ parameters at M_{SUSY} in SPheno

As in the case of SARAH, the $\overline{\rm MS}$ parameters are first shifted to $\overline{\rm DR}$ parameters and the SUSY thresholds are added at $Q = M_{\rm SUSY}$. The main difference is that the conservation of $\mathrm{SU}_L(2)\times U_Y(1)$ is assumed at this scale. The corresponding formulae read

1. **Gauge couplings**: these get shifted by

$$\left(g_i^{\overline{\rm DR}}\right)^2 = \frac{(g_i^{\overline{\rm MS}})^2}{1-\frac{(g_i^{\overline{\rm MS}})^2}{8\pi^2}\Delta g_i^2} \tag{A.47}$$

where

$$\begin{aligned}\Delta g_1^2 = -\sum_{i=1}^{3}\Bigg[&\frac{1}{12}\log\left(\frac{m_{L_i}^2}{Q^2}\right)+\frac{1}{12}\log\left(\frac{m_{E_i}^2}{Q^2}\right)\\ &+\frac{1}{36}\log\left(\frac{m_{Q_i}^2}{Q^2}\right)\\ &+\frac{1}{18}\log\left(\frac{m_{D_i}^2}{Q^2}\right)+\frac{2}{9}\log\left(\frac{m_{U_i}^2}{Q^2}\right)\Bigg]\\ &-\frac{1}{12}\log\left(\frac{m_H^2}{Q^2}\right)-\frac{1}{3}\log\left(\frac{|\mu|^2}{Q^2}\right)\end{aligned} \tag{A.48}$$

$$\begin{aligned}\Delta g_2^2 = \frac{1}{3}-\sum_{i=1}^{3}\Bigg[&\frac{1}{12}\log\left(\frac{m_{L_i}^2}{Q^2}\right)+\frac{1}{4}\log\left(\frac{m_{Q_i}^2}{Q^2}\right)\Bigg]\\ &-\frac{1}{12}\log\left(\frac{m_H^2}{Q^2}\right)-\frac{1}{3}\log\left(\frac{|\mu|^2}{Q^2}\right)\\ &-\frac{2}{3}\log\left(\frac{|M_2|^2}{Q^2}\right)\end{aligned} \tag{A.49}$$

$$\begin{aligned}\Delta g_3^2 = \frac{1}{2}-\frac{1}{12}\sum_{i=1}^{3}\Bigg[&2\log\left(\frac{m_{Q_i}^2}{Q^2}\right)+\log\left(\frac{m_{D_i}^2}{Q^2}\right)\\ &+\log\left(\frac{m_{U_i}^2}{Q^2}\right)\Bigg]-\log\left(\frac{|M_3|^2}{Q^2}\right),\end{aligned} \tag{A.50}$$

and m_{L_i}, m_{E_i}, m_{Q_i}, m_{D_i} and m_{U_i} are the masses of the $\tilde{L}$, $\tilde{E}$, $\tilde{Q}$, $\tilde{D}$ and $\tilde{U}$, respectively, calculated from the corresponding soft SUSY breaking mass squares. m_H is the mass of the heavy Higgs boson, which is calculated according to

$$\begin{aligned}m_H^2 = \frac{1}{2}\Big(&M_{H_u}^2+M_{H_d}^2+|\mu|^2\\ &+\sqrt{(M_{H_u}^2-M_{H_d}^2)^2+4|B\mu|^2}\Big).\end{aligned} \tag{A.51}$$

2. **Yukawa couplings:** First the shift from $\overline{\rm MS}$ to $\overline{\rm DR}$ is calculated according to

$$Y_{{\rm SM},l}^{\overline{\rm DR}\,\prime} = \left(1-\frac{3}{128\pi^2}\left(g_1^2-g_2^2\right)\right)Y_{{\rm SM},l}^{\overline{\rm MS}}, \tag{A.52}$$

$$Y_{{\rm SM},d}^{\overline{\rm DR}\,\prime} = \left(1-\frac{13g_1^2}{1152\pi^2}+\frac{3g_2^2}{128\pi^2}-\frac{g_3^2}{12\pi^2}-\frac{43g_3^4}{9(16\pi^2)^2}\right)Y_{{\rm SM},d}^{\overline{\rm MS}}, \tag{A.53}$$

$$Y_{{\rm SM},u}^{\overline{\rm DR}\,\prime} = \left(1-\frac{7g_1^2}{1152\pi^2}+\frac{3g_2^2}{128\pi^2}-\frac{g_3^2}{12\pi^2}-\frac{43g_3^4}{9(16\pi^2)^2}\right)Y_{{\rm SM},u}^{\overline{\rm MS}},$$

(A.54)

where the gauge couplings g_i are the $\overline{\rm DR}$ couplings. In a second step, these couplings get rescaled as follows:

$$Y^{\overline{\rm DR}}_{{\rm SM},l} = \frac{1}{\cos\beta} Y^{\overline{\rm DR}\,\prime}_{{\rm SM},l}\,,\ ,\ Y^{\overline{\rm DR}}_{{\rm SM},d} = \frac{1}{\cos\beta} Y^{\overline{\rm DR}\,\prime}_{{\rm SM},d}\,,\ ,\ Y^{\overline{\rm DR}}_{{\rm SM},u} = \frac{1}{\sin\beta} Y^{\overline{\rm DR}\,\prime}_{{\rm SM},u}\,. \tag{A.55}$$

In the next step, the one-loop corrections due to the SUSY particles and the heavy Higgs doublet H, where H is to the SM-Higgs orthogonal combination of H_u and H_d. Here we distinguish between holomorphic and non-holomorphic corrections, where the first denotes loop contributions to the existing tree-level coupling and the second the loop-induced ones to the second Higgs doublet. We give here for simplicity the different contributions for the case of real parameters neglecting flavour mixing. The case with flavour mixing can easily be obtained from Appendix A, see Ref. [84].

– Taking either $f = t$ or $f = b$ we obtain for the gluino contributions

$$Y^{\rm hol}_f = \frac{g_3^2}{6\pi^2} M_3 T_f C_0(M_3^2, m_Q^2, m_F^2), \tag{A.56}$$

$$Y^{\rm anhol}_f = -\frac{g_3^2}{6\pi^2} M_3 Y_f \mu C_0(M_3^2, m_Q^2, m_F^2). \tag{A.57}$$

– Taking either $f = t$, $f = b$ or $f = \tau$ we obtain for the single bino contributions

$$Y^{\rm hol}_f = c_f \frac{g_1^2}{16\pi^2} M_1 T_f C_0(M^2 13, m_{L_f}^2, m_F^2), \tag{A.58}$$

$$Y^{\rm anhol}_f = -c_f \frac{g_1^2}{16\pi^2} M_1 Y_f \mu C_0(M_1^2, m_{L_f}^2, m_F^2), \tag{A.59}$$

where $L_f = Q$ in the case of $f = t, b$ and $L_f = L$ in the case $f = \tau$ and the different combinations of hypercharges give

$$c_t = -\frac{2}{9}\ ,\ c_b = \frac{1}{9}\ ,\ c_\tau = -1. \tag{A.60}$$

– Taking either $f = t$ or $f = b$ we obtain for the single higgsino contributions

$$Y^{\rm hol}_f = \frac{Y_t Y_b}{16\pi^2} \mu^2 Y_{f'} C_0(\mu^2, m_Q^2, m_{F'}^2), \tag{A.61}$$

$$Y^{\rm anhol}_f = -\frac{Y_t Y_b}{16\pi^2} \mu T_{f'} C_0(\mu^2, m_Q^2, m_{F'}^2), \tag{A.62}$$

where $f' = b\ (t)$ in the case of $f = t\ (b)$.

– For the mixed wino/higgsino contributions we find

$$Y^{\rm hol}_f = -\frac{3}{4}\frac{g_2^2}{16\pi^2} Y_f C_2(M_2^2, \mu^2, m_{L_f}^2), \tag{A.63}$$

$$Y^{\rm anhol}_f = \frac{3}{4}\frac{g_2^2}{16\pi^2} \mu M_2 Y_f C_0(M_2^2, \mu^2, m_{L_f}^2), \tag{A.64}$$

with $L_f = Q$ in the case of $f = t, b$ and $L_f = L$ in the case $f = \tau$.

– For the mixed bino/higgsino contributions we find

$$Y^{\rm anhol}_f = -\frac{g_1^2}{16\pi^2} Y_f \left(c_{fL} C_2(M_2^2, \mu^2, m_{L_f}^2) + c_{fR} C_2(M_2^2, \mu^2, m_F^2)\right), \tag{A.65}$$

$$Y^{\rm anhol}_f = \frac{g_1^2}{16\pi^2} \mu M_1 Y_f \left(c_{fL} C_0(M_2^2, \mu^2, m_{L_f}^2) + c_{fR} C_0(M_2^2, \mu^2, m_F^2)\right), \tag{A.66}$$

with $L_f = Q$ in the case of $f = t, b$ and $L_f = L$ in the case $f = \tau$. For the different coefficients we obtain

$$c_{tL} = c_{bL} = \frac{1}{6}\ ,\ c_{tR} = \frac{2}{3}\ ,\ c_{bR} = -\frac{1}{3}\ ,\ c_{\tau L} = -\frac{1}{2}\ ,\ c_{\tau R} = 1\,. \tag{A.67}$$

– The contributions due to the second heavy Higgs doublet with mass m_H read

$$Y^{\rm hol}_f = c_f \frac{Y_f^3}{16\pi^2} \ln\left(\frac{m_H^2}{M_{\rm SUSY}^2}\right) \tag{A.68}$$

where $c_f = \sin^2\beta$ in the case of $f = b, \tau$ and $c_f = \cos^2\beta$ in the case of $f = t$.

In the case of the u-type quarks a simple summation of all contributions suffices,

$$Y_u = Y^{\overline{\rm DR}}_{{\rm SM},u} - \Delta Y^{\rm hol}_u - \Delta Y^{\rm anhol}_u \cot\beta. \tag{A.69}$$

In the case of the d-type quarks and the leptons one has to resum the anholomorphic contributions as they get large in the case of large $\tan\beta$,

$$Y_f = \frac{Y^{\overline{\rm DR}}_{{\rm SM},f}}{1 + \frac{\Delta Y^{\rm anhol}_f}{Y^{\overline{\rm DR}}_{{\rm SM},f}} \tan\beta} - \Delta Y^{\rm hol}_f \tag{A.70}$$

where $f = d$. For completeness we note that the equivalence of the resummation of the two-point function (as in the case of SARAH) with the resummation of the three-point function (as in SPheno) has been shown in [85].

The loop functions are given by

$$C_0(m_1^2, m_2^2, m_3^2) = \frac{1}{m_2^2 - m_3^2}\left[\frac{m_2^2}{m_1^2 - m_2^2}\ln\left(\frac{m_2^2}{m_1^2}\right) - \frac{m_3^2}{m_1^2 - m_3^2}\ln\left(\frac{m_3^2}{m_1^2}\right)\right], \tag{A.71}$$

$$C_2(m_1^2, m_2^2, m_3^2) = \ln\left(\frac{m_3^2}{M_{\rm SUSY}^2}\right) + \frac{m_2^4}{(m_3^2 - m_2^2)(m_2^2 - m_1^2)} \times \ln\left(\frac{m_3^2}{m_2^2}\right) - \frac{m_1^4}{(m_3^2 - m_1^2)(m_2^2 - m_1^2)}\ln\left(\frac{m_3^2}{m_1^2}\right). \tag{A.72}$$

Appendix B Using the new and old approach in SARAH/SPheno

Appendix B.1 SARAH

The new matching routines and Higgs mass calculations are available with SARAH version 4.9.0. By default, the new routines are included in the SARAH output of the SPheno source code for any model. Moreover, they are also used by default now for supersymmetric models with the following restriction: SARAH only calculates the effective Higgs pole mass within the SM, if the second lightest CP-even scalar has a pole mass above 500 GeV. The reason is that one expects for lighter mass splitting potential important effects from the mixing between the two lightest scalars which would get lost in the effective model ansatz. In addition, there are the following flags which can be used by the user in the LesHouches input file to control when the calculations shall be performed:

```
Block SPHENOINPUT #
...
66  1  # Two-scale matching (yes/no)
67  1  # Calculate Higgs mass in effective SM if possible (yes/no/always)
```

The options can be used as follows:

66

0 the old one-scale matching is used;
1 the new two-scale matching is used.

The default value is 1

67

0 the Higgs mass is only calculated at the SUSY scale in the full model;
1 the Higgs mass is calculated in the effective SM if only one light scalar is present;
2 the Higgs mass is always calculated in the effective SM even if light scalars are present.

The default value is 1.

Appendix B.1 SPheno

In SPheno the new matching procedure and Higgs mass calculation is available with version 4.0.0 and higher. This procedure is by default switched on but one can switch back to the old one-scale matching using the new entry 49 in block SPHENOINPUT

```
Block SPHENOINPUT #
...
48  1  # 0.. 2-loop QCD to Y_t and alpha_s at m_Z, 1 ... use fit formula at 3 loop
49  1  # Two-scale matching 0/1 correspond to yes/no
```

where the value 1 switches to the one-scale matching. Using three-loop fit formulas given in [42] instead of the two-loop corrections to $Y_t^{\overline{\rm MS}}$ and one-loop corrections to α_s at m_Z can be achieved by setting the new flag 48 in block SPHENOINPUT to 1. Moreover, the entry 38 controlling the order used in the RGEs has been modified.

```
Block SPHENOINPUT #
...
38  3  # 1 & 2: use 1- and 2-loop RGEs; 3: 3-loop SM RGE and 2-loop SUSY RGEs
```

with the options

1 one-loop RGEs for both SM and SUSY;
2 two-loop RGES for both SM and SUSY;
3 three-loop RGEs for SM but two-loop RGEs for SUSY.

References

1. ATLAS Collaboration, G. Aad et al., Phys.Lett. **B716** (2012), 1–29. arXiv:1207.7214
2. Cms, S. Chatrchyan et al. Phys. Lett. B **716**, 30–61 (2012). arXiv:1207.7235
3. ATLAS Collaboration, , Tech. Report ATLAS-CONF-2016-052, CERN, Geneva, Aug 2016
4. ATLAS Collaboration, , Tech. Report ATLAS-CONF-2016-054, CERN, Geneva, Aug 2016
5. ATLAS Collaboration, , Tech. Report ATLAS-CONF-2016-078, CERN, Geneva, Aug 2016
6. CMS Collaboration, S. Xie, , Tech. Report CMS-CR-2016-241, CERN, Geneva, Oct 2016
7. B. Allanach, A. Bednyakov, R.R. de Austri, Comput. Phys. Commun. **189**, 192–206 (2015). doi:10.1016/j.cpc.2014.12.006
8. T. Hahn, S. Heinemeyer, W. Hollik, H. Rzehak, G. Weiglein, Comput. Phys. Commun. **180**, 1426–1427 (2009)

9. S. Heinemeyer, W. Hollik, G. Weiglein, Comput. Phys. Commun. **124**, 76–89 (2000). arXiv:hep-ph/9812320
10. T. Hahn, S. Heinemeyer, W. Hollik, H. Rzehak, G. Weiglein, Phys. Rev. Lett. **112**(14), 141801 (2014). arXiv:1312.4937
11. J. Pardo Vega, G. Villadoro, JHEP **07**, 159 (2015). arXiv:1504.05200
12. P. Athron, J.-H. Park, T. Steudtner, D. Stöckinger, A. Voigt, JHEP **01**, 079 (2017). arXiv:1609.00371
13. H. Bahl, W. Hollik, Eur. Phys. J. C76(9), 499 (2016). arXiv:1608.01880
14. J.R. Espinosa, M. Quiros, Phys. Lett. B **266**, 389–396 (1991)
15. N. Arkani-Hamed, S. Dimopoulos, JHEP **06**, 073 (2005). [arXiv:hep-th/0405159]
16. G.F. Giudice, A. Romanino, Nucl. Phys. **B699**, 65–89 (2004). [arXiv:hep-ph/0406088], [Erratum: Nucl. Phys.B706,487(2005)]
17. G.F. Giudice, A. Strumia, Nucl. Phys. B **858**, 63–83 (2012). arXiv:1108.6077
18. G. Degrassi, S. Di Vita, J. Elias-Miro, J.R. Espinosa, G.F. Giudice, G. Isidori, A. Strumia, JHEP **08**, 098 (2012). arXiv:1205.6497
19. P. Draper, G. Lee, C.E.M. Wagner, Phys. Rev. D **89**, 055023 (2014). arXiv:1312.5743
20. E. Bagnaschi, G.F. Giudice, P. Slavich, A. Strumia, JHEP **09**, 092 (2014). doi:10.1007/JHEP09(2014)092
21. H.E. Haber, R. Hempfling, Phys. Rev. D **48**, 4280–4309 (1993). arXiv:hep-ph/9307201
22. M.S. Carena, J. Espinosa, M. Quiros, C. Wagner, Phys. Lett. B **355**, 209–221 (1995). arXiv:hep-ph/9504316
23. G. Lee, C.E.M. Wagner, Phys. Rev. D 92(7), 075032 (2015). arXiv:1508.00576
24. N. Arkani-Hamed, S. Dimopoulos, G.F. Giudice, A. Romanino, Nucl. Phys. B **709**, 3–46 (2005). arXiv:hep-ph/0409232
25. W. Kilian, T. Plehn, P. Richardson, E. Schmidt, Eur. Phys. J. C **39**, 229–243 (2005). arXiv:hep-ph/0408088
26. N. Bernal, A. Djouadi, P. Slavich, JHEP **0707**, 016 (2007). arXiv:0705.1496
27. W. Porod, Comput. Phys. Commun. **153**, 275–315 (2003). arXiv:hep-ph/0301101
28. W. Porod, F. Staub, Comput. Phys. Commun. **183**, 2458–2469 (2012). arXiv:1104.1573
29. F. Staub, (2008). arXiv:0806.0538
30. F. Staub, Comput. Phys. Commun. **181**, 1077–1086 (2010). arXiv:0909.2863
31. F. Staub, Comput. Phys. Commun. **182**, 808–833 (2011). arXiv:1002.0840
32. F. Staub, Comput. Phys. Commun. **184**, 1792–1809 (2013). arXiv:1207.0906
33. F. Staub, Comput. Phys. Commun. **185**, 1773–1790 (2014). arXiv:1309.7223
34. F. Staub, Adv. High Energy Phys. **2015**, 840780 (2015). arXiv:1503.04200
35. B. Allanach, Comput. Phys. Commun. **143**, 305–331 (2002). arXiv:hep-ph/0104145
36. B. Allanach, M. Bernhardt, Comput. Phys. Commun. **181**, 232–245 (2010). arXiv:0903.1805
37. B.C. Allanach, P. Athron, L.C. Tunstall, A. Voigt, A.G. Williams, Comput. Phys. Commun. **185**, 2322–2339 (2014). arXiv:1311.7659
38. A. Djouadi, J.-L. Kneur, G. Moultaka, Comput. Phys. Commun. **176**, 426–455 (2007). arXiv:hep-ph/0211331
39. D.M. Pierce, J.A. Bagger, K.T. Matchev, R.-J. Zhang, Nucl. Phys. B **491**, 3–67 (1997). arXiv:hep-ph/9606211
40. J. Baglio, R. Gröber, M. Mühlleitner, D.T. Nhung, H. Rzehak, M. Spira, J. Streicher, K. Walz, Comput. Phys. Commun. **185**(12), 3372–3391 (2014). arXiv:1312.4788
41. P. Athron, J.-H. Park, D. Stöckinger, A. Voigt, Comput. Phys. Commun. **190**, 139–172 (2015). doi:10.1016/j.cpc.2014.12.020
42. D. Buttazzo, G. Degrassi, P.P. Giardino, G.F. Giudice, F. Sala, A. Salvio, A. Strumia, JHEP **12**, 089 (2013). arXiv:1307.3536
43. S. Weinberg, Phys. Lett. B **91**, 51–55 (1980)
44. L.J. Hall, Nucl. Phys. B **178**, 75–124 (1981)
45. E.A. Bagnaschi et al., Eur. Phys. J. C **75**, 500 (2015). arXiv:1508.01173
46. K.L. Chan, U. Chattopadhyay, P. Nath, Phys. Rev. D **58**, 096004 (1998). arXiv:hep-ph/9710473
47. J.L. Feng, K.T. Matchev, T. Moroi, Phys. Rev. Lett. **84**, 2322–2325 (2000). arXiv:hep-ph/9908309
48. J.L. Feng, K.T. Matchev, T. Moroi, Phys. Rev. D **61**, 075005 (2000). arXiv:hep-ph/9909334
49. J.L. Feng, K.T. Matchev, F. Wilczek, Phys. Lett. B **482**, 388–399 (2000). arXiv:hep-ph/0004043
50. G.G. Ross, K. Schmidt-Hoberg, F. Staub, JHEP **03**, 021 (2017). doi:10.1007/JHEP03(2017)021
51. H. Bahl, KUTS workshop (2017). https://docs.google.com/viewer?a=v&pid=sites&srcid=ZGVmYXVsdGRvbWFpbnxrdXRzbWh8Z3g6NzA1NDUzZGYwMjljOTQyNw
52. W. Porod, F. Staub, A. Vicente, Eur. Phys. J. C **74**(8), 2992. doi:10.1140/epjc/s10052-014-2992-2
53. M.D. Goodsell, K. Nickel, F. Staub, Eur. Phys. J. C **75**(1), 32 (2015). arXiv:1411.0675
54. M. Goodsell, K. Nickel, F. Staub, Eur. Phys. J. C **75**(6), 290 (2015). arXiv:1503.03098
55. M.D. Goodsell, F. Staub, Eur. Phys. J. **C 77**(1), 46 (2017). arXiv:1604.05335
56. S.P. Martin, Phys. Rev. D **65**, 116003 (2002). arXiv:hep-ph/0111209
57. S.P. Martin, Phys. Rev. D **67**, 095012 (2003). arXiv:hep-ph/0211366
58. S.P. Martin, Phys. Rev. D **70**, 016005 (2004). arXiv:hep-ph/0312092
59. S.P. Martin, Phys. Rev. D **68**, 075002 (2003). arXiv:hep-ph/0307101
60. S.P. Martin, Phys. Rev. D **71**, 116004 (2005). arXiv:hep-ph/0502168
61. M.D. Goodsell, K. Nickel, F. Staub, Phys. Rev. D **91**, 035021 (2015). arXiv:1411.4665
62. F. Staub, P. Athron, U. Ellwanger, R. Gröber, M. Mühlleitner, P. Slavich, A. Voigt, Comput. Phys. Commun. **202**, 113–130 (2016). arXiv:1507.05093
63. S.P. Martin, Phys. Rev. D **89**, 013003 (2014). arXiv:1310.7553
64. S.P. Martin, Phys. Rev. **D90**(1), 016013 (2014). arXiv:1406.2355
65. J. Braathen, M.D. Goodsell, JHEP **12**, 056 (2016). arXiv:1609.06977
66. J. Braathen, M.D. Goodsell, F. Staub
67. U. Ellwanger, C. Hugonie, A.M. Teixeira, Phys. Rept. **496**, 1–77 (2010). arXiv:0910.1785
68. B. O'Leary, W. Porod, F. Staub, JHEP **05**, 042 (2012). arXiv:1112.4600
69. M. Hirsch, M. Malinsky, W. Porod, L. Reichert, F. Staub, JHEP **1202**, 084 (2012). arXiv:1110.3037
70. M. Hirsch, W. Porod, L. Reichert, F. Staub, Phys. Rev. D **86**, 093018 (2012). arXiv:1206.3516
71. J.E. Camargo-Molina, B. O'Leary, W. Porod, F. Staub, JHEP **12**, 103 (2013). arXiv:1309.7212
72. N. Blinov, D.E. Morrissey, JHEP **03**, 106 (2014). arXiv:1310.4174
73. D. Chowdhury, R.M. Godbole, K.A. Mohan, S.K. Vempati, JHEP **02**, 110 (2014). arXiv:1310.1932
74. J.E. Camargo-Molina, B. Garbrecht, B. O'Leary, W. Porod, F. Staub, Phys. Lett. B **737**, 156–161 (2014). arXiv:1405.7376
75. J. Beuria, U. Chattopadhyay, A. Datta, A. Dey, JHEP **4**, 024 (2017). doi:10.1007/JHEP04(017)024
76. S. Fanchiotti, B.A. Kniehl, A. Sirlin, Phys. Rev. D **48**, 307–331 (1993). arXiv:hep-ph/9212285

77. G. Degrassi, S. Fanchiotti, A. Sirlin, Nucl. Phys. B **351**, 49–69 (1991)
78. J.A. Grifols, J. Sola, Nucl. Phys. B **253**, 47 (1985)
79. P.H. Chankowski, A. Dabelstein, W. Hollik, W.M. Mosle, S. Pokorski, J. Rosiek, Nucl. Phys. B **417**, 101–129 (1994)
80. L.V. Avdeev, MYu. Kalmykov, Nucl. Phys. B **502**, 419–435 (1997). arXiv:hep-ph/9701308
81. A. Bednyakov, A. Onishchenko, V. Velizhanin, O. Veretin, Eur. Phys. J. C **29**, 87–101 (2003). arXiv:hep-ph/0210258
82. J. Fleischer, F. Jegerlehner, O.V. Tarasov, O.L. Veretin, Nucl. Phys. **B539**, 671–690 (1999). arXiv:hep-ph/9803493, [Erratum: Nucl. Phys.B571,511(2000)]
83. R. Harlander, P. Kant, L. Mihaila, M. Steinhauser, JHEP **09**, 053 (2006). arXiv:hep-ph/0607240
84. A.J. Buras, P.H. Chankowski, J. Rosiek, L. Slawianowska, Nucl. Phys. B **659**, 3 (2003). arXiv:hep-ph/0210145
85. M. Carena, D. Garcia, U. Nierste, C.E.M. Wagner, Nucl. Phys. B **577**, 88–120 (2000). arXiv:hep-ph/9912516